

# Strategic Environment: Conservation Policies Effectiveness and Strategic Behavior

Preliminary draft

Angelo Santos \*

April 7, 2025

## Abstract

In this paper, I evaluate the environmental impacts of a conservation project funded by USAID in Eastern Zambia, which established protected areas within contracted chiefdom boundaries in partnership with local authorities. Leveraging satellite and administrative data merged at the 1km × 1km grid level from 2001 to 2023, I employ a Difference-in-Differences strategy to estimate the program's effects on deforestation across distinct regional groups. The results indicate a significant reduction in tree cover loss within Protected Areas, though no overall impact is observed at the chiefdom level. There is no evidence of leakage to Non-Protected Areas; however, I find positive spillover effects in Non-Contracted Chiefdoms located near protection boundaries. Heterogeneity analysis reveals that conservation effects were more pronounced in areas with greater infrastructure access and human presence. Additionally, I document selection bias in the placement of Protected Areas, which were more likely to be located in remote regions with lower baseline deforestation. These findings underscore the importance of accounting for spatial targeting and incentive structures in the design of effective conservation policies.

---

\* Angelo Santos: Department of Economics, University of Houston, Houston, Texas, USA ([afdos-san@cougarnet.uh.edu](mailto:afdos-san@cougarnet.uh.edu)). I want to thank professor Katharine Baldwin for kindly allowing me to use her data on chiefdom boundaries. I also thank USAID for allowing me to use the CFP project dataset. The views and opinions expressed in this paper are those of the author and not necessarily the view and opinion of the United States Agency for International Development. This paper is part of the project "Climate Risk, Pollution, and Childhood Inequalities in Low- and Middle-income Countries," which is supported by National Science Foundation Grant 2230615 (PI: Hannum)

## 1 Introduction

From 2001 to 2022, there was a total of 459 Mha of tree cover loss globally (12% decrease) and 195 Gt of CO emissions. Related to it, according to Watson, Schalatek, and Evéquoz (2020) deforestation accounts for 12% - 20% of the global Greenhouse gas emissions (GHG). These gases include different types of pollutants such as CO<sub>2</sub>, NO<sub>2</sub>, and SO<sub>2</sub>, which contribute to temperature rise and air pollution. Another negative side of these gases is the impact on human development outcomes, such as health, mortality, and cognitive development. To reduce deforestation rates, policymakers have been designing different types of interventions to incentivize pro-environmental behavior, which needs to compensate for forgone income due to deforestation activities (Jayachandran 2022; Jack et al. 2022). This is especially relevant in regions where a considerable share of households are dependent on forest-related activities such as wood product production, charcoal, or cleaning forests for subsistence agriculture (Cisneros et al. 2022; Correa et al. 2020).

In this paper, I evaluate the impact of a REDD+ project implemented by USAID in Eastern Zambia on deforestation, focusing on communal land management. To do so, I construct a high-resolution panel dataset at the 1km × 1km grid level spanning from 2001 to 2023 by integrating administrative records and geospatial data. I incorporate detailed information from USAID on newly established Protected Areas and the classification of Chiefdoms as Contracted or Non-Contracted. These data are merged with satellite-based measures of tree cover and forest loss from Hansen et al. (2013). Additionally, I compile a range of geospatial covariates, including agricultural land productivity, settlement locations, altitude, and distances to key infrastructure such as roads, water bodies, and the electrical grid. To account for long-term political and institutional boundaries, I also link this dataset to historical pre-colonial chiefdom boundaries from Baldwin (2013).

The empirical strategy relies on a Difference-in-Differences (DiD) framework to estimate the program's effect on annual deforestation rates. The baseline specification compares grid cells located within the Luangwa Corridor—an ecologically significant area targeted by the program—with those outside the corridor. To capture within-chiefdom variation, I distinguish between Protected and Non-Protected areas within Contracted Chiefdoms. This allows me to test for heterogeneous treatment effects and potential leakage resulting from differential conservation incentives. I further explore potential spillover effects by examining deforesta-

tion trends in Non-Contracted Chiefdoms that are geographically close to Protected Areas. In addition, I analyze heterogeneous effects conditional on grid-level characteristics and assess potential selection bias in the siting of Protected Areas by comparing pre-treatment characteristics of Protected and Non-Protected grids.

Zambia has the 4th largest forest in Africa and has been facing a worrying increase in deforestation patterns in the last few years. The country has the 12th highest deforestation rate in the world, and 4th in per capita terms (Global Forest Watch). These increased threats reduced Zambian tree cover by approximately 9.4 % in the last 20 years, mainly driven by land clearing for agriculture, wood extraction, and charcoal production (USAID 2016). In 2015, USAID implemented the Community Forests Project (CFP) in partnership with BioCarbon Partners signing contracts with chiefdom to conserve areas within their boundaries. The protected areas serve as a benchmark for carbon offsets that are sold and generate revenues that are used to invest in community projects within contracted Chiefdoms.

Even though there is extensive literature analyzing different conservation policies, how to better design conservation policies is an open question as multiple factors can influence the effectiveness of these policies (Balboni et al. 2023; Jayachandran 2022). For instance, take-up is a crucial element for the success of these initiatives, but what impacts conservation take-up is still lacking in evidence. Papers have shown how institutional dimensions such as trust in contract realization, corruption, and political representation can influence program takeup and effectiveness (Burgess et al. 2012; Cisneros and Kis-Katos 2022; Jack et al. 2022; Gulzar, Lal, and Pasquale 2024). Another relevant dimension is land property rights, as agents' incentives to protection are closely related to who will receive the benefits of conservation efforts (Baragwanath and Bayi 2020, Sze et al. 2022 Baland et al. 2010). The amount of the financial incentives is an important aspect of these programs considering the compensation for the opportunity costs of not deforesting. Land usage models incorporate the maximization process in choosing to engage in environmentally destructive activities, such as the benefits of forests for communities or the benefits of land change for agriculture production. This cost of not deforesting can be related to different aspects such as forest income dependence, and skill formation cost to work with non-forest services. The long-term takeup is also relevant for the sustainability element of PES programs. These projects demand considerable funding to compensate agents for pro-environmental behaviors, the end of financial support may lead agents to return to activities that will destroy the environment which questions the long-term effects

of these interventions.

I aim to contribute to the literature in the following dimensions. First, I am the first to evaluate this project, which is the biggest REDD+ project in the African continent. Second, I aim to add the literature on understanding how community pay-for-performance (PES) programs can incentivize conservation in the context of communal lands (Sims 2010; Malan et al. 2024). Communal land is an important setting as this is a feature present in countries where land ownership is related to historical or ethnic origins, such as Chiefdoms in African countries or Native land demarcations in Latin America. Third, I investigate selection bias in the designation of protected areas in the context of chiefdom-owned lands. The endogenous nature of the REDD+ area designation allows me to understand how local authorities may strategically allocate locations that are less costly to conserve. Fourth, I explore the program's spillover effects on Non-Protected and neighboring Areas, by estimating the effects on Non-Contracted Chiefdoms.

The results of this paper indicate no significant overall effect of the program on annual tree cover loss at the chiefdom level. However, I find consistent evidence of reduced deforestation within the boundaries of Protected Areas (PAs), suggesting that conservation efforts were effective in the designated zones. Importantly, there is no evidence of leakage, i.e., increased deforestation—in nearby Non-Protected areas. The analysis also reveals selection bias in the decision of Protected Areas designation, which were more likely to be established in regions with lower pre-policy deforestation rates and greater remoteness. This finding highlights the importance of accounting for the incentives created by conservation policy design. Because program payments were tied to avoided deforestation within the protected boundaries, local decision-makers may have had an incentive to select areas with already low deforestation pressure in order to maximize performance with minimal intervention.

Moreover, I find evidence of positive spillover effects: areas adjacent to protection boundaries also experienced a reduction in deforestation after the policy was implemented. The heterogeneity analysis shows that the largest post-policy reductions occurred in areas closer to roads and human settlements, suggesting that conservation efforts were particularly effective in regions facing higher deforestation pressure. These results indicate that while the program successfully reduced deforestation within and near Protected Areas, its overall impact was constrained by strategic site selection, which favored low-risk areas. This highlights the importance of designing conservation programs that align incentives with broader envi-

ronmental goals.

The rest of this paper is organized as follows. Section 2 provides additional information on the CFP program and institutional background in Zambia. Section 3 describes the datasets used in the analysis and presents summary statistics for the grids across Non-Contracted Chiefdoms, and Contracted Chiefdoms. Section 4 outlines the empirical strategy and Section 5 presents the results. Finally, the paper concludes with final remarks in Section 6.

## 2 Institutional Background

In 2015, USAID launched the Community Forests Program (CFP) in Eastern Zambia aiming to reduce gas emissions due to deforestation. The project cost approximately 16 million USD dollars to be implemented and was done in partnership with BioCarbon Partners, a firm specializing in forest conservation projects. The project aimed to protect a natural corridor called the Luangwa Valley, where there is an important biodiversity presence (Figure ??). According to USAID (2019), the intervention successfully institutionalized a minimum of 700,000 protected hectares within the valley. They aimed to create a long-term contract relationship with Chiefdoms that committed to protecting areas within the corridor. Using estimations of stored carbon and avoided emissions due to the intervention in protected areas, the firm sold carbon offsets in the voluntary market. The income obtained from carbon offsets is reinvested in infrastructure and mitigation activities in communities within the contracted chiefdom.

The project took place in Eastern Zambia, where the majority of the households lack service access and are socioeconomically vulnerable. According to USAID (2016), 87.4 % of the population live in rural areas and do not have access to electricity, public water, or sanitation. Subsistence agriculture is an important component of household income, composing up to 64 % of it. Another important source of income is charcoal production, which is used for electricity, forest product production, and cooking by Zambian families. These families are economically vulnerable with 75 % of them living with less than \$1.5 per day, and 60 % live in extreme poverty. This highlights how these communities are dependent on forest usage for income, household activities, and nutrition, a clear challenge to the program's success.

The contract was established at the chiefdom level in partnership with chiefs, government agencies, and local authorities. The chiefdom REDD+ protected areas (Figure ??) were delimited after an extensive interaction with local communities and authorities to determine what areas would be protected and measured in order to measure the carbon offsets. These

contracts have a period of 30 years and aim to create a long-term relationship with chiefdoms. During these years, the program committed to selling carbon-verified credits and reinvesting the revenue in projects that would benefit the communities. The carbon verification was established in 2019 and sold carbon-verified credits corresponding to the 5 years from the beginning of the program (2015-2019). After that, the carbon verification will happen in a year manner until the end of the 30-year contract in 2045. This component can potentially lead to a long-term incentive to conserve the protected areas, as the conservation revenue will keep being reinvested into communities.

To incentivize conservation in non-protected areas, the program financed basic infrastructure and livelihood income alternatives. The funds for the project are transferred to Chiefdoms which decide the allocation of these resources through local administration boards called Community Resources Board (CRBs) and Village Action Groups (VGAs). The chiefdom authorities then decided how to invest the resources in their communities. The program restricted the investments to the provision of physical infrastructure or financing of mitigation activities that aimed to create alternatives to forest products and non-sustainable activities such as crop burning.

In terms of investments in infrastructure, the program financed multiple types of physical benefits. For example, building schools, water distribution systems, boats for Ecotourism, and trucks for forest monitoring. These resources were provided to the communities conditional on local demands and chiefdom negotiations. For livelihood income alternatives, the project funds non-forest activities aiming to reduce the need for deforestation and forest degradation. The activities include bee-keeping, Eco-charcoal, Ecotourism, and smart agriculture. For example, the bee-keeping project distributed hives to communities to allow them to produce honey without extracting this from forests. Another type of income alternative, the Eco charcoal technique, allows families to reduce forest degradation by being more selective on the tree type and tools for its extraction. The agriculture initiative includes techniques that reduce land degradation and still allow communities to produce crops but in a more sustainable manner. It is important to note that there is no additional incentive for conservation in non-protected areas, these incentives aim to support families in a transition to less forest-dependent income sources.

### 3 Data

#### 3.1 USAID datasets

In 2015, USAID conducted baseline surveys that included 324 villages and 4,343 households across six different chiefdoms, five of which entered into contracts with the program. The endline dataset was completed in June 2024 and includes additional information on treatment types, such as cash transfer amounts and specific activities provided by the program. These surveys also contain geocoded information regarding the locations of villages and households, allowing me to map these communities.

Additionally, a structured survey interview was conducted with the headperson (traditional leader) of each village in the study area. The current headperson, whether at baseline or endline, was selected for the survey across all 324 communities. Village leaders provided information on whether the program was implemented in their village and if they received any benefits from it. For household heads, the survey also asked whether they received benefits from the program, such as participation in program activities, employment in ecotourism, or infrastructure improvements received by the village. Using this information, I was able to identify villages that received benefits within treated chiefdoms.

#### 3.2 Zambia data

**Chiefdom boundaries** For defining the chiefdom boundaries, I use the shapefile from Baldwin (2013)<sup>1</sup>, which geocodes the limits of the chiefdoms based on historical pre-colonial maps of the region. This shapefile provides an essential geographical foundation, ensuring that the spatial delineation of chiefdoms reflects historically accurate boundaries with cultural and political significance. By using these geocoded boundaries, I can align contemporary data with historically rooted geographic divisions.

The geocoded chiefdom boundaries are particularly valuable for examining institutional and environmental outcomes across different regions. These boundaries allow for a more precise analysis of localized governance and resource management, especially about forest dependence and agricultural practices. Additionally, they facilitate the integration of spatial data with household-level survey information, enabling a comprehensive examination of

---

1. More details on the methodology and sources used to create the chiefdom boundaries can be found in Baldwin (2015), which provides a deeper exploration of the pre-colonial era maps and their relevance to modern governance structures.

how historical chiefdom boundaries influence present-day outcomes.

### 3.3 Satellite data

**Tree coverage data.** To measure deforestation rates, I use the Global Forest Watch dataset (Hansen et al. 2013), which provides information for  $30m \times 30m$  raster points. I use two layers from this dataset: cell share of tree cover share and year of tree cover loss. I aggregate raster points to grids of approximately  $1km \times 1km$  (0.01-degree). Figure 3a illustrates the raw measures of tree cover in the baseline for the Eastern Region, for the Hansen cells' share of tree cover. And Figure 3b maps the tree cover loss in 2023; this figure displays red cells indicating tree cover loss in 2023. Using these two layers I can compute my tree cover measurements.

The first layer is the baseline share of tree cover for 2000, which measures the share of forest canopy at the cell level. The dataset defines a tree as any vegetation taller than 5 meters in height. Following this definition, the author verifies the proportion of a cell covered by forest canopy—the upper layer or “roof” of a forest, formed by the crowns of trees—and assigns this value to the cell. A limitation of this definition is the possibility of including plantations that meet these criteria, such as timber plantations, in my forest cover measurements. For each cell, Hansen et al. (2013) reports the share of the unit covered by the forest canopy, ranging from 0 to 100.

The second layer reports tree cover loss at the cell level. According to Hansen et al. (2013), forest loss is defined as a stand-replacement disturbance or the complete removal of tree canopy cover at the Landsat pixel scale. This means I am unable to track the gradual degradation of tree cover in a particular cell. For example, if a cell has a 50% tree cover, I cannot track if this decreases to 20% in a particular period and then to zero in another subsequent year. The Hansen dataset only indicates whether the cell was fully deforested in a given year. Tree loss at the cell level is recorded as a numerical variable, indicating the year when the cell lost its tree cover. Values range from 0 to 23, where 0 indicates no loss, and 1 to 23 represents the year of loss starting from 2001. Using the annual information on tree cover loss, I can create yearly deforestation measures.

One limitation of these measurements is the inability to track tree cover gains after 2000. This means that if a cell experiences an increase in tree cover after 2000, this will not be reflected in my measurements. Additionally, a cell that undergoes multiple changes, such as deforestation, reforestation, and deforestation again, will not have these variations captured

by my deforestation measure.

**Tree cover measurement.** To define a particular Hansen cell as forested I use a canopy share threshold  $\alpha$ . For example, if  $\alpha$  is equal to 10, only cells with more than 10 percent of their area covered by forest canopy will be considered to calculate the tree cover measurements. Formally, consider a set of locations  $i = 1, 2, \dots, n$  with  $n$  being the total number of locations considered. Each location  $i$  has  $j$  grids defined by latitude and longitude coordinates  $lat_j, long_j$  that are within its location boundaries  $b_i$  such that:

$$\begin{aligned} lat_{i,\text{Min}} &\leq lat_j \leq lat_{i,\text{Max}} \\ \text{and} \\ lon_{i,\text{Min}} &\leq lon_j \leq lon_{i,\text{Max}} . \end{aligned} \tag{3.1}$$

Each of these cells  $j$  has a canopy share  $cs_{j,2000}$  in the baseline year 2000. With this I can define canopy share  $cs_i$  in a particular location  $i$  conditional on canopy share threshold  $\alpha$  using the following:

$$cs_{i,2000}(\alpha) = \left( \frac{\sum_{j \in b_i} \mathbb{1}\{cs_{j,2000} > \alpha\}}{\sum_{j \in b_i} \mathbb{1}\{j \in b_i\}} \right) . \tag{3.2}$$

Intuitively, this equation states that forest share of a geographical location can be obtained by a simple ratio. The numerator is the sum of cells with canopy share above a specific threshold  $\alpha$  and that overlap with location  $i$  boundaries. The denominator is the number of cells within the location boundaries. In my case, this corresponds to the share of forested cells within a  $1\text{km} \times 1\text{km}$  grid  $i$ .

**Deforestation measurements.** Using the tree cover and year of loss, I can obtain the annual deforested cells for a specific geographical unit. I will measure this in two different ways: Share of area deforested relative to the forest stock in 2000 and the share of area deforested relative to the forest stock in the previous year. I use the same notation as before, but add a new element to incorporate the possibility of deforestation per year. Let  $tl_{j,y}$  be the binary variable equal to 1 if a particular cell  $j$  loses its tree cover in year  $y$ , zero otherwise. I will also use a threshold  $\alpha$  to limit the cells used in our deforestation measurement. I.e, the relevant cells for the calculation are the ones with canopy share above a specific threshold  $\alpha$ . For example, if I want to calculate the deforestation rate considering forest canopy share bigger than 10 %, the cell considered in both the denominator and numerator of the deforestation rate calculation are above this threshold. Using this notation, I calculate location  $i$  newly deforested cells in

year  $y$  ( $i_y$ ). Formally :

$$d_{iy} = \sum_{j \in b_i} \mathbb{1}\{tl_{jy} = 1\} \cdot \mathbb{1}\{cs_{j,2000} > \alpha\} \times cs_{j,2000} . \quad (3.3)$$

This measures the number of Hansen cells  $j$  with canopy share bigger than  $\alpha$  and deforested in year  $y$  within each 1 km grid  $i$ . To consider the initial tree cover area within each 1 km block, I calculate location  $i$  deforestation rate relative to year  $r$  ( $D_{iy}^r$ ) conditional on cell canopy share threshold  $\alpha$  as follows:

$$D_{iy}^r (\alpha) = \left( \frac{\sum_{j \in b_i} \mathbb{1}\{tl_{jy} = 1\} \cdot \mathbb{1}\{cs_{j,2000} > \alpha\}}{\sum_{j \in b_i} \mathbb{1}\{cs_{j,2000}^r > \alpha\}} \right) . \quad (3.4)$$

In the numerator I compute the number of cells deforested at location  $i$ , and in the denominator, I compute the total number of cells categorized as forested in 2000 in year  $r$ . Both the numerator and denominator consider a threshold  $\alpha$  for cell canopy share. I compute the deforestation rate relative to 2000 -  $r = 2000$  - and to the previous year -  $r = t - 1$ . The deforestation relative to 2000 can be computed as follows :

$$D_{iy}^{2000} (\alpha) = \left( \frac{\sum_{j \in b_i} \mathbb{1}\{tl_{jy} = 1\} \cdot \mathbb{1}\{cs_{j,2000} > \alpha\}}{\sum_{j \in b_i} \mathbb{1}\{cs_{j,2000}^{2000} > \alpha\}} \right) . \quad (3.5)$$

Which measures the proportion of the cover observed in 2000 that is lost in a particular year. This measure is informative of how much grids are deforesting relative to the same year, which is not impacted by the nonidentification of reforestation that may happen after 2000. However, this measure does not reflect that losing 1 unit of forest cell can be very different when the stock of trees is getting close to zero. The deforestation rate relative to the previous year can reflect that. This can be computed as follows :

$$D_{iy}^{t-1} (\alpha) = \left( \frac{\sum_{j \in b_i} \mathbb{1}\{tl_{jy} = 1\} \cdot \mathbb{1}\{cs_{j,2000} > \alpha\}}{\sum_{j \in b_i} \mathbb{1}\{cs_{j,2000}^{t-1} > \alpha\}} \right) . \quad (3.6)$$

In this measure, the denominator is updated every year by subtracting lost cells in the year before. This imply that the same number of deforested cells will reflect a higher deforestation rate compared to  $D_{iy}^{2000}$ , reflecting a higher weight to each unit deforested as forest stock decreases. I show results using both measures.

Figure 4 display the distribution of tree cover share for Grids 1km×1km obtained by

aggregating Hansen cells in different chiefdoms. The mean for these observations ranges between 18% and 28%, which categorizes very sparse vegetation as this region is characterized by savannas.

**Supplementary data** To enrich the grid-level analysis, I constructed several geospatial covariates using a variety of publicly available datasets. These include: distance to settlements (km), distance to roads (km), distance to water bodies (km), distance to the electrical network (km), altitude (meters), and land productivity. Distance measures were calculated through spatial operations that compute the Euclidean distance from each grid centroid to the nearest feature in the respective shapefiles. Road and water body shapefiles were obtained from the OpenStreetMap project, while data on the electrical network was sourced from a World Bank project focused on Zambia. Settlement data comes from the GRID3 ZMB – Settlement Extents v3.0 dataset, which provides high-resolution polygons and centroid coordinates for settlements across Zambia. Altitude was derived using grid coordinates in combination with elevation data from open-access global terrain datasets. Finally, land productivity was measured using data from the FAO’s Global Agro-Ecological Zones (GAEZ) project, specifically the agro-climatic potential yield for maize—the most commonly cultivated crop in the study region. These variables are used to control for geographic and agricultural heterogeneity in deforestation outcomes.

### 3.4 Summary Statistics

Table 1 provides summary statistics for all Grids located within Game Management Areas (GMAs) in Zambia, splitting these observations into five groups. The first column presents statistics for observations that are outside the Luangwa Corridor and are used as controls for the analysis. The second column shows statistics for observations within Non-Contracted Chiefdoms but within the Corridor. The Third column presents observations within contracted Chiefdoms, located in protected (PA) or non-protected areas (NPA), which are shown separately in columns 3 and 4.

The first row shows the average grid canopy share in 2000, indicating the average percentage of tree canopy cover in each grid by different location groups. The units of observation do not differ substantially in terms of tree cover across all five groups. Within contracted chiefdoms, protected areas have around 1.3 % more tree cover compared to non-protected areas. This suggests that blocks are not substantially different in terms of the density of trees, i.e.,

protected areas or contracted chiefdoms are not more forested areas in comparison to non-contracted areas.

However, notable differences can be observed on tree cover loss statistics between 2001 and 2014. Non-Contracted Chiefdom deforested on average around 2000 m<sup>2</sup> per grid relative to Chiefdoms included in the program. The control groups also display higher tree cover loss, around 3000 m<sup>2</sup> more tree cover loss per grid. Another considerable difference exists between Protected Areas and Non-Protected areas. PAs deforested areas are on average 5 times less than areas not included in the protection boundaries. These simple comparisons reveal that the program delimited low deforestation areas, potentially influenced by the local authorities' endogenous choice of protection boundaries. This pattern has been found in other localities where conservation policies took place. (Giudice et al. 2019; Cisneros et al. 2022).

On the geographical characteristics, non-contracted chiefdoms and controls are situated slightly higher, compared to 707.82 meters in participant chiefdoms. Locations show similar potential for maize yield varying from approximately 3170 kg/ha to 2979 kg/ha across all groups.

Another significant difference particular to Protected areas (PAs) is the significant remoteness. These grids are more remote compared to non-protected areas when considering their proximity to human settlements, roads, and energy networks. On average, blocks within PAs are located 5.3 km, 9.1 km, and 70 km farther from these infrastructures, respectively. These differences in remoteness are particularly relevant to understanding deforestation dynamics, as infrastructure availability has been shown to play a crucial role in facilitating agricultural activities and contributing to tree cover loss (Gollin and Wolfersberger 2024).

In summary, grids are similar in tree cover density and geographical characteristics but differ in terms of deforestation patterns and distance to infrastructure. Contracted chiefdom annual tree cover loss is smaller in comparison to Chiefdoms not included in the program, and Protected Areas tend to experience less deforestation and are more remote compared to Non-protected areas.

## 4 Estimation Strategy

**Contracted Chiefdom outcomes** The program signed contracts with selected chiefdoms in which conservation was incentivized by rewarding communities for the preservation of trees. After consultations with local authorities, protected areas were delineated within these Chief-

doms boundaries, where the stock of tree would be monitored and valued in terms of stored carbon. The revenue from sold carbon offsets would be reinvested in the Chiefdom through infrastructure and mitigation activities to reduce forest-service dependence. Economic incentive theory suggests that Non-Protected areas, where presentation is not rewarded, may experience increasing tree cover loss due to the reallocation of deforestation pressure from protected areas. Which can offset the conservation efforts implemented within the delineated areas. To test the overall effect of the program on the overall Chiefdom conservation, I first examine the effects in grids within treated chiefdoms, without considering their protection status after the program. Next, I split the Contracted chiefdoms into protected and Non-Protected grids to separate possible conservation and leakage effects after program implementation. The comparison group for this analysis consists of grid-level data from non-treated Chiefdoms located outside the Luangwa Valley. Figure 5 illustrates the geographical distribution of these groups.

The choice of a control group outside these regions aims to reduce possible spillover concerns related to Non-Contracted Chiefdoms close to the program implementation. Due to conservation efforts from Contracted chiefdoms, as patrol monitoring, other areas can be impacted by the program by the enforcement of the preservation efforts in the area. Another hypothesis is the increase in the incentives for deforesting in neighboring locations, as these communities can take advantage of a possible supply reduction of forest-related products as charcoal. Another important restriction in my sample is the location of a Grid within a Game Management Area, this decision is based on the fact that land usage laws are different across protection types. Zambia is divided into National Parks, Game Management Areas, and Forest Reserves, which differ substantially in the restriction on tree cover reduction. National Parks are federally owned and have zero tolerance for deforestation and has no human presence, whereas GMAs and Forest Reserves do allow for it. For my analysis, I will use GMAs only to avoid concerns with the differences in natural resources governance.

To estimate the program's effect on Chiefdom's annual deforestation rate, I use a Difference-in-Differences (DiD) approach leveraging grid-level information (Abman and Lundberg 2024; Cisneros et al. 2022). The assumption for causal identification is that the deforestation rates would maintain the same trend in the absence of the program for Chiefdoms that received the USAID contract and those outside the region. I will run the following regression:

$$D_{ict}^r = \alpha + \beta After_t \cdot Contracted_c + \eta_t + \delta_c + \epsilon_{ict} \quad (4.1)$$

In this equation,  $D_{ict}^r$  corresponds to the annual deforestation rate measured relative to  $r$  for Grid  $i$  in Chiefdom  $c$  at year  $t$ .  $After_t$  is a dummy variable equal to 1 if year  $t$  is after 2014, when the program started.  $Contracted_c$  indicates if Chiefdom  $c$  is included in the CFP contract.  $\beta_1$  captures the effect of the program for grids within treated Chiefdoms. I use time ( $\eta_t$ ) and chiefdom ( $\delta_c$ ) fixed effects to control for time-invariant unobservable characteristics related to Chiefdom and particular year that may impact tree cover loss.  $\epsilon_{ict}$  is an idiosyncratic error term, and errors are clustered at the chiefdom level to account for serial correlation between observations.

To estimate the yearly effects of the program and to test the parallel trends assumption for the Contracted Chiefdom sample, I estimate the following event study:

$$D_{ict}^r = \alpha + \sum_k \beta_k \mathbb{1}(t = k) Contracted_c + \eta_t + \delta_c + \epsilon_{ict}. \quad (4.2)$$

In this equation,  $D_{ict}^r$  corresponds to the annual deforestation rate measured relative to  $r$  for Grid  $i$  in Chiefdom  $c$  at year  $t$ . I regress this on yearly coefficients ( $\beta_k$ ) before and after the program implementation. The coefficients will give me the yearly effects of the program on annual deforestation outcomes. To control for time-invariant unobservable characteristics that impact deforestation rates, I use time ( $\delta_t$ ) and chiefdom ( $\gamma_c$ ) fixed effects. I add an idiosyncratic error term  $\epsilon_{ict}$  and I clustered errors at the chiefdom level to account for serial correlation.

To investigate whether the differential incentives given to communities concerning preservation in Protected Areas and Non-Protected Areas, I estimate the impact of the program for these two groups. I create a dummy variable ( $Protected_i$ ) which is equal to 1 if an observation lies within the protected areas. I also include a dummy ( $Non-Protected_i$ ) for grids outside the Protected Areas and within the Contracted Chiefdoms. The identification assumption relies on the parallel trends between these two groups and controls outside the corridors. The Difference in Differences equation is the following:

$$D_{ict}^r = \alpha + \beta_1 After_t \cdot Protected_i + \beta_2 After_t \cdot Non-Protected_i + \lambda Protected_i + \eta_t + \delta_c + \epsilon_{ict}. \quad (4.3)$$

This equation is similar to 4.1, but splitting  $Contracted_c$  into  $Protected_i$  and  $Non-Protected_i$ .  $\beta_1$  captures the conservation effect of the program in the Protected Areas, whereas  $\beta_2$  captures the leakage effect of the program in the Non-Protected Areas. The coefficient  $\lambda$  adjusts for pre-

treatment differences between the two groups. As previously stated, I include fixed effects, and cluster errors at the Chiefdom level.

To test for parallel trends and yearly effects for these two groups, I estimate the following:

$$D_{ict}^r = \alpha + \sum_k \beta_k \mathbb{1}(t = k) \text{Protected}_i + \sum_k \gamma_k \mathbb{1}(t = k) \text{Non-Protected}_i + \lambda \text{Protected}_i + \eta_t + \delta_c + \epsilon_{ict} . \quad (4.4)$$

In this event study,  $\beta_k$  captures the yearly effects of the program in Protected Areas, and  $\gamma_k$  captures the yearly effects of the program in the Non-Protected Areas. The statistical insignificance of the coefficients before the program implementation indicates parallel trends and that the coefficients from 4.3 can be interpreted as causal.

**Spillover Effects on Non-Contracted Chiefdoms** The intervention aimed to incentivize conservation within Chiefdoms that signed contracts with USAID. However, the delineated Protected Areas are adjacent to other Chiefdoms in the Luangwa Valley corridor that did not participate in the program. These neighboring Chiefdoms may experience spillover effects, either through enforcement activities such as patrol monitoring, or due to shifts in deforestation incentives. For instance, forest-dependent households in Non-Contracted Chiefdoms may respond to changes in the supply of forest-related products like charcoal or timber, potentially leading to increased forest exploitation. To investigate whether the conservation program induced such externalities, I estimate the program's effects on deforestation rates in Non-Contracted Chiefdoms located within the corridor.

Following a similar approach to the analysis of Contracted Chiefdoms (4.1), I first estimate the average effect of the program for grids within Non-Contracted Chiefdoms using a Difference-in-Differences (DiD) specification:

$$D^{rict} = \alpha + \beta \text{After}_t \cdot \text{Non-Contracted}_c + \eta_t + \delta_c + \epsilon_{ict} . \quad (4.5)$$

In this equation,  $D_{ict}^r$  represents the annual deforestation rate for grid  $i$  in Chiefdom  $c$  at year  $t$ , relative to  $r$ . The variable  $\text{Non-Contracted}_c$  indicates whether a Chiefdom is located within the corridor but was not included in the program. The interaction term captures the potential spillover effect of the program on these Chiefdoms ( $\beta$ ). I include year ( $\eta_t$ ) and Chiefdom ( $\delta_c$ )

fixed effects, and cluster standard errors at the Chiefdom level.

To explore the dynamic effects and validate the parallel trends assumption, I estimate the following event study specification:

$$D^{rict} = \alpha + \sum_k \beta_k \mathbb{1}(t = k) Non-Contracted_c + \eta_t + \delta_c + \epsilon_{ict}. \quad (4.6)$$

This equation estimates yearly effects of the program in Non-Contracted Chiefdoms relative to the baseline period, 2014. Insignificant coefficients in the pre-program period would support the parallel trends assumption, allowing for causal interpretation of post-treatment coefficients.

To explore heterogeneity in spillover effects within Non-Contracted Chiefdoms, I classify grids based on their proximity to the nearest Protected Area. I define two groups: Close grids, located < than 60 km from the boundary of Protected Areas, and Far grids, located beyond this threshold. This allows me to examine whether spillovers are more pronounced in areas closer to the intervention. Figure 5b illustrates the geographical distribution of these groups. The DiD specification is:

$$D^{rict} = \alpha + \beta_1 After_t \cdot Close_i + \beta_2 After_t \cdot Far_i + \lambda Close_i + \eta_t + \delta_c + \epsilon_{ict}. \quad (4.7)$$

In this regression,  $\beta_1$  captures the spillover effect in Close grids, and  $\beta_2$  captures the effect in Far grids. The coefficient  $\lambda$  adjusts for pre-treatment differences between the two groups. As in previous models, I include fixed effects and cluster errors at the Chiefdom level.

Finally, I estimate an event study to capture the yearly evolution of spillover effects by distance to the program boundaries:

$$D^{rict} = \alpha + \sum_k \beta_k \mathbb{1}(t = k) Close_i + \sum_k \lambda_k \mathbb{1}(t = k) Far_i + \lambda Close_i + \eta_t + \delta_c + \epsilon_{ict}. \quad (4.8)$$

Here,  $\beta_k$  measures yearly effects for Close grids, while  $\lambda_k$  measures effects for Far grids. Pre-treatment insignificance would support the parallel trends assumption, while post-treatment differences reveal the extent and timing of spatial spillovers.

**Selection of protected areas and Matching samples** The selection of protected areas within Contracted Chiefdoms was carried out in collaboration with the conservation firm BioCarbon Partners, based on a validation process that confirmed chiefdom boundaries and land tenure

arrangements. However, this selection process was not random and may have introduced bias on site selection. Because program revenues were linked to avoided carbon emissions within the Protected Areas, local authorities had a potential incentive to prioritize areas with low baseline deforestation pressure to maximize conservation gains while minimizing the actual effort required. This form of strategic selection may threaten the causal interpretation of the program impacts as trends may not be parallel due pre-existing land-use patterns. To investigate the selection bias on site selection, I follow the approach of Cisneros et al. (2022) and estimate a Logit model to examine the likelihood of a grid cell being included in a Protected Area, conditional on grid-characteristics. The estimated equation is as follows:

$$\text{Protected}_{ic} = \alpha + X'_{ic}\beta + \epsilon_{ic} . \quad (4.9)$$

In this model,  $\text{Protected}_{ic}$  is a dummy variable that equals 1 if the cell  $i$  is included in the protected areas of chiefdom  $c$ , as determined by the intervention.  $X_{ic}$  is a vector of characteristics of the grids related to the likelihood of being protected. This includes the average deforestation rate before the policy started, tree cover in 2000, altitude, distance to human settlements, distance to water bodies, distance to roads, distance to electricity network, distance to National Parks and a measure of potential corn yields. This model is estimated using the sample of grids within Contracted Chiefdoms.

**Matching sample** After estimating the likelihood of a grid cell being designated as protected using Equation 4.9, I use the estimated coefficients to compute a propensity score for each grid cell in the sample. This score reflects the probability that a grid is protected, conditional on its geospatial characteristics. Using these scores, I implement a Nearest Neighbor matching algorithm without replacement to identify one matched control grid for each treated (protected) grid. The matched cells are found among observations outside the Corridor to avoid spillovers concerns. The intuition behind this procedure is to find places that would be likely assigned to be Protected if these Chiefdoms received the program.

Figure 6 displays the resulting matched samples across the four previously defined groups: Protected, Non-Protected, Close, and Far. To illustrate how different potential controls and Gridis within the corridors might be, I plot the Propensity score distribution across these groups, before and after the matching procedure. Figure 7 shows these distributions for Protected and Non-Protected Areas. Two key insights can be observed here. First, Potential

controls presents a distribution with higher concentration of observations on the left side. This indicates that when using this as control group for Protected Areas, the comparison include Grids with low probability of being Protected. Second the matching procedure is able to overlap propensity score distributions for both groups, as seen in Figures 7b and 7d. Figure 8 plots the distributions for the close and far Grids within Non-Contracted Chiefdoms.

It is important to highlight that the analysis leverages the parallel trends assumption. While this approach does not require strict exogeneity and, allows for selection into treatment, it relies on the idea that similar grids are likely to exhibit similar pre-treatment trends. By controlling for observable geospatial characteristics in the propensity score model, I aim to capture key dynamics related to deforestation and improve the validity of comparisons between treated and control units.

## 5 Results

In this section, I present the results on the impact of the policy intervention on tree cover loss. I begin by analyzing overall deforestation trends at the chiefdom level, focusing on areas that entered into conservation contracts (Contracted Chiefdoms). Next, I examine the program's differential effects on protected versus non-protected areas within these contracted regions. I then explore potential spillover effects in neighboring chiefdoms that did not participate in the program (Non-Contracted Chiefdoms). Finally, I assess how the program's impact varies based on grid-level characteristics, shedding light on potential sources of heterogeneity in treatment effects.

**Contracted Chiefdoms** The estimates of the effect of the program on Contracted Chiefdom annual deforestation rate is illustrated in Table 2. I estimate regressions (4.1) and (4.3) using two different outcomes measures, the annual deforestation rate relative to 2000 ( $D^{2000}$ ), and relative to the previous year ( $D^{t-1}$ ). I split the table in two parts to illustrate the sample difference. Columns 1 to 4 presents results using the raw sample of potential controls outside the corridors (Figure 5a), and Columns 5 to 8 using the matched samples (Figures 6a and 6b).

The table shows a consistent pattern of conservation effects on Protected areas, reducing the annual deforestation rate of tree cover loss. When using the raw sample as comparison group, I find that there is a reduction of 0.119 percentage points on the deforestation rate relative to forest stock in 2000. This coefficient is more negative when using the annual deforesta-

tion relative to the previous year, indicating a reduction of 0.146 percentage points. The same pattern can be observed when comparing with the matched sample, but the magnitudes are bigger. The results indicates that Protected Areas have 0.16 percentage points reduction in its annual deforestation rate relative to 2000, 0.187 relative to the previous year.

However, no leakage effects on Non-Protected regions and overall impact at the Chiefdom level is observed as all the coefficients are statistically insignificant. The absence of leakage can be due two things. First, Protected Areas were not intensively used by Chiefdoms, as shown in table 1, which explains why deforestation leakage should be small if any. The heterogeneous effects analysis, shown later, indicates that the program effects were driven by the reduction on deforestation rates close to roads and villages. As the Protected Areas are hard to access and low populated regions, agents that were restricting theirs forest activities after the program may be constrained on their capacity to deforest outside the Protection boundaries. However, if they do start deforesting more on Non-Protected Areas, the proportion of this event may not be enough to change the region deforestation trends after policy. Another explanation is the compensation through implementation of mitigation activities within the Chiefdom. Agents living in Contracted chiefdoms may be able to acquire income from non-deforesting services financed by the program as forest patrol, eco tourism, and bee-keeping production, which may reduced their incentives on tree cover loss.

The parameters discussed before can be interpreted as causal if the parallel trends assumption holds, indicating that contracted and non-contracted chiefdom areas outside the corridor would follow the same trend in the absence of the program. The event study results from Equation (4.2) and (4.4) can be seen in Figures 9, 10, and ???. These figures shows that both the deforestation rate relative to 2000 and previous yes display a very similar pattern in terms of coefficient magnitudes and significance. The matched sample have coefficients before police more concentrated around the zero line, indicating a improving in the parallel trends assumptions visualization. The yearly coefficients after the policy implementation suggest that the reduction in annual deforestation rate observed in Protected Areas is statistically significant after 2018. This is an important result as the program started the payment of yearly revenues from carbon offsets in 2019. This may have brought to communities benefits and trust improvement on the contract, incentivizing consistent conservation.

**Non Contracted Chiefdoms** Similarly to the estimates on Contracted Chiefdoms, Table 3 presents these estimates for Non-Contracted Chiefdoms. I estimate regressions (4.5) and (4.7)

using two different outcomes measures, the annual deforestation rate relative to 2000 ( $D^{2000}$ ), and relative to the previous year ( $D^{t-1}$ ). I split the table in two parts to illustrate the sample difference. Columns 1 to 4 presents results using the raw sample of potential controls outside the corridors (Figure 5b), and Columns 5 to 8 using the matched samples (Figures 6c and 6d). The table shows a consistent pattern of conservation effects on areas close to the Protected areas, indicating a positive spillover on reducing the annual deforestation rate of tree cover loss. No effects is observed for far samples and overall impact at the Chiefdom level.

I observe conservation spillover on Closer areas, reducing the annual deforestation rate of tree cover loss. The raw sample sample results shows a reduction of 0.1 percentage points on the deforestation rate relative to forest stock in 2000, which is slightly more negative when using the annual deforestation relative to the previous year, -0.128. When comparing with the matched sample, the magnitudes are bigger. Closer Areas have 0.157 percentage points reduction in its annual deforestation rate relative to 2000, 0.186 relative to the previous year. This suggests that the implementation of the program in the corridor may have induced conservation in the neighbor areas. One hypothesis is the increase in monitoring and enforcement from Contracted Chiefdoms, which can have behaved as a protector of the region. Another explanation can be knowledge share between these regions which may have led them to transition to less forest-depedent services and products. No overall effects on Non-Contracted Chiefdoms is observed, and regions located at least 60 km from the Protection boundaries do not present differential effects.

I plot event study coefficients on Non-Contracted Chiefdoms Areas in Figures 9, 13, and 12. These figures aim to investigate if these locations were facing parallel trends in deforestation rate compared to the comparison group outside the corridor. These coefficients come from Equation (4.6) and (4.8) previously described. As seen before for contracted chiefdoms, deforestation rate relative to 2000 and previous yes display a very similar pattern in terms of coefficient magnitudes and significance. The matched sample also display better parallel trend, with coefficients concentrated around zero. The pattern of reduction after 2018 is the same as protected areas, indicating that neighbor regions are following similar patterns.

**Heterogeneous Effects** Figure 14 presents event study estimates examining the heterogeneous effects of the policy. The analysis is disaggregated by protection status (Protected vs. Non-Protected grids) and proximity to PAs. The dependent variables include my two deforestation measures: baseline tree cover in 2000 ( $D^{2000}$ ) and relative to the previous year ( $D^{t-1}$ ).

Figures 14a and 14b focus on Contracted Chiefdoms. Protected grids have statistically insignificant coefficient associated to proximity from PA borders, and mean tree cover in 2000. This suggests that the program did not have a differential impact for more forested grids and those relative more remote relative to the Protection borders. However, I find differential effects for distances to roads and settlements, reaffirming the role of accessibility on deforestation dynamics. The coefficient associated to settlement proximity indicates that the program was less effective in more remote places, associating one additional km farther to a coefficient of 0.02 percentage points smaller for the deforestation rate reduction. Additionally, one km farther from roads associated with a smaller reduction in deforestation rate of 0.009 and 0.007 percentage points. This indicates that the effects of the program are driven by grids that are closer to villages and road access, indicating the conservation effects on places with deforestation pressure. For Non-Protected areas, no estimates were found significantly different to zero.

Figures 14c and 14d present results for Non-Contracted Chiefdoms located within 60 km of protected grids and farther. In these regions, the estimates indicate significant associations between distance to the Protection borders and to roads. This pattern is consistent with positive spillover effects from nearby protection efforts, indicating that the conservation spillover effects fade with distance to PAs. Distance to roads continues to be associated with smaller effects (0.009 and 0.011 percentage points) of the program on deforestation, reinforcing the importance of infrastructure access in shaping land-use change.

Overall, the results underscore two key insights. First, proximity to PAs appears to generate deforestation reductions even in adjacent non-contracted areas, and this effect dissipates with distance. Second, proximity to roads and settlements are consistently correlated with higher deforestation. The heterogeneous effects of the program indicates that conservation was driven by reduction tree loss close to roads, human settlement and the border of protected areas.

## 6 Conclusion

This paper investigates the impacts of a large-scale REDD+ conservation program implemented by USAID and BioCarbon Partners in Eastern Zambia, the biggest REDD+ project in Africa. I aimed to understand how conservation incentives operate in regions where land governance is based on customary institutions, and to what extent such interventions can effectively reduce

deforestation while avoiding unintended consequences like leakage.

To conduct this analysis, I construct a novel geospatial panel dataset at a high spatial resolution ( $1\text{km} \times 1\text{km}$ ) spanning from 2001 to 2023. I combine remote sensing data on tree cover and forest loss with administrative information on newly established protected areas, historical chiefdom boundaries, and various environmental and infrastructural variables. The empirical strategy employs a Difference-in-Differences framework that exploits variation across time and space—comparing trends before and after the program’s implementation within and across Contracted, Non-Contracted and control chiefdoms. I further disaggregate Chiefdoms by separating Protected and Non-Protected areas within Contracted Chiefdoms, and also explore potential spillovers into neighboring non-contracted regions. Heterogeneous effects are examined based on proximity to infrastructure, settlement density, and land characteristics.

The analysis yields several important findings. First, I find no significant overall effect of the program on deforestation at the chiefdom level, suggesting that the aggregate impact of the intervention is limited. However, a more granular analysis reveals strong conservation effects within the formally Protected Areas: annual tree cover loss decreased significantly after implementation. These conservation gains, though, are offset by evidence of strategic site selection—Protected Areas were disproportionately located in remote regions with lower baseline deforestation pressure, indicating that local decision-makers may have prioritized easier-to-protect zones in anticipation of performance-based payments.

Importantly, I do not find evidence of negative leakage into nearby Non-Protected Areas within the same contracted chiefdoms. On the contrary, the results suggest a decline in deforestation close to protection boundaries, indicating potential positive spillovers. The heterogeneous effects analysis also shows that the strongest conservation effects occurred in areas closer to infrastructure and human settlements, where deforestation pressures are typically higher. This implies that the program was most effective in regions with a greater need for intervention—provided those regions were included within protected boundaries.

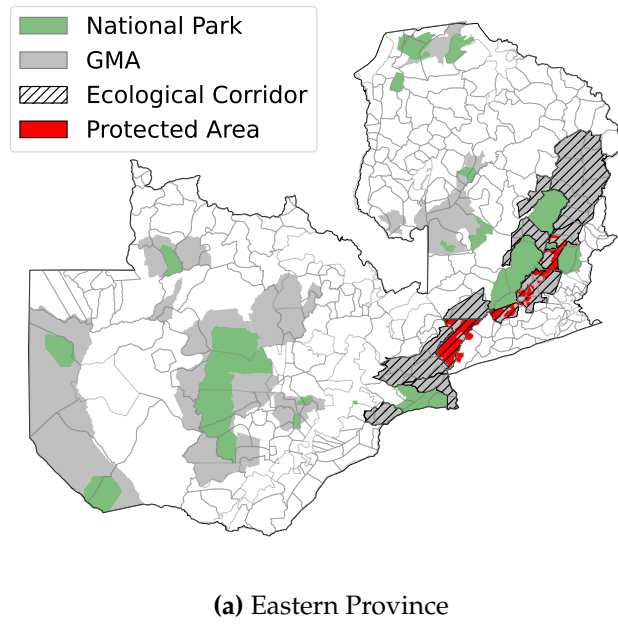
These findings carry important policy implications. First, they highlight the potential for REDD+ programs to achieve localized conservation gains, especially when implemented with robust monitoring and enforcement mechanisms. However, the evidence of strategic targeting and the lack of significant aggregate effects point to a need for improved incentive structures—ensuring that protection efforts are directed toward high-threat areas rather than low-cost, low-risk zones. Additionally, the observed positive spillovers suggest that program

influence can extend beyond strictly defined intervention boundaries, which should be considered in program design and evaluation.

Overall, this study contributes to the broader literature on environmental policy, land governance, and the design of conservation incentives. It underscores the importance of integrating spatial heterogeneity, local governance dynamics, and behavioral responses into evaluations of conservation programs. Future REDD+ initiatives should carefully consider not only where interventions take place but how site selection decisions interact with underlying land-use pressures and incentive mechanisms.

## Tables and Figures

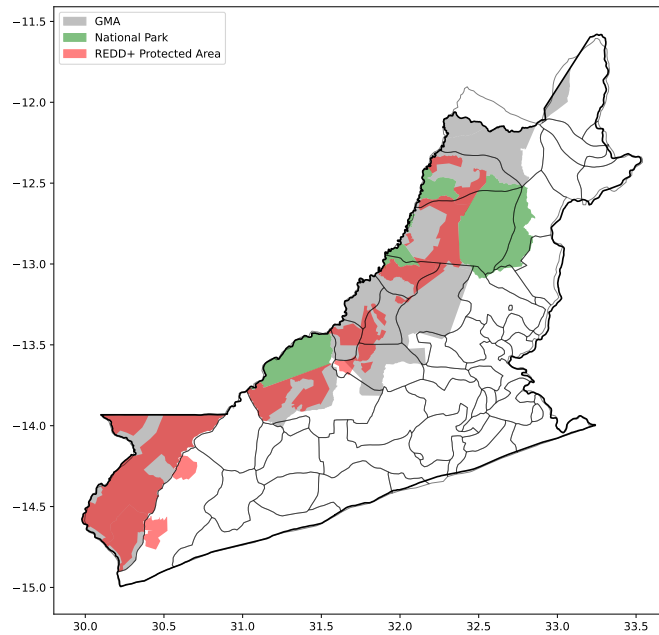
**Fig. 1.** Game Management Areas, National Parks and REDD+ Protected areas in Zambia



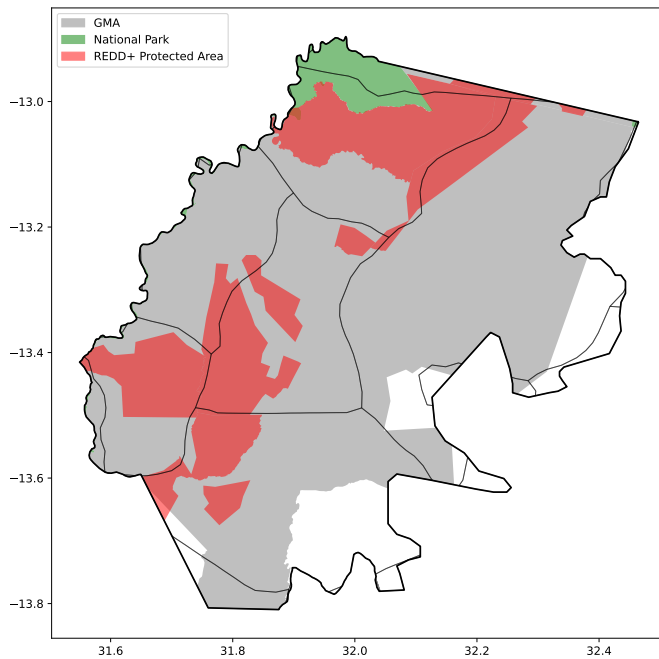
**(a)** Eastern Province

*Note: This map shows Zambia and its chiefdom boundaries with additional layers of Game Management Areas (GMAs), National Parks, and REDD+ Protected areas in Zambia. The green layer represents the Natural Parks, the gray layer shows the GMAs and the red layer indicates the protected areas defined by the REDD+ program. The hatched area indicates the Luangwa Valley, an important biodiversity location in Eastern Zambia, targeted by the program.*

**Fig. 2.** Conservation areas in Eastern Province and Mambwe District



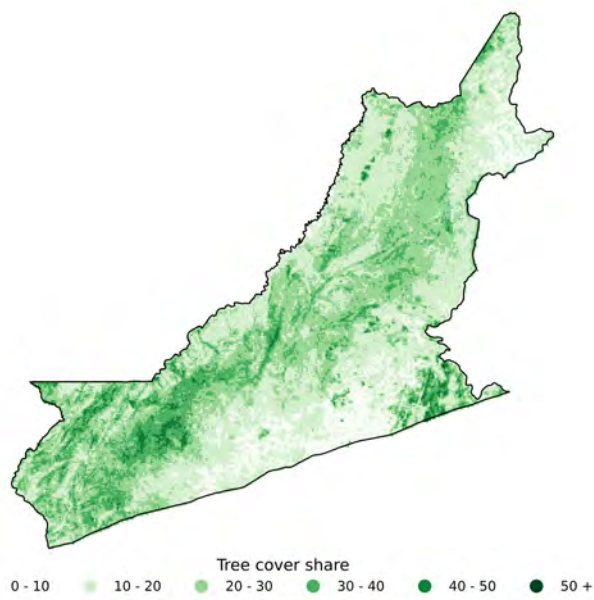
**(a)** Eastern Province



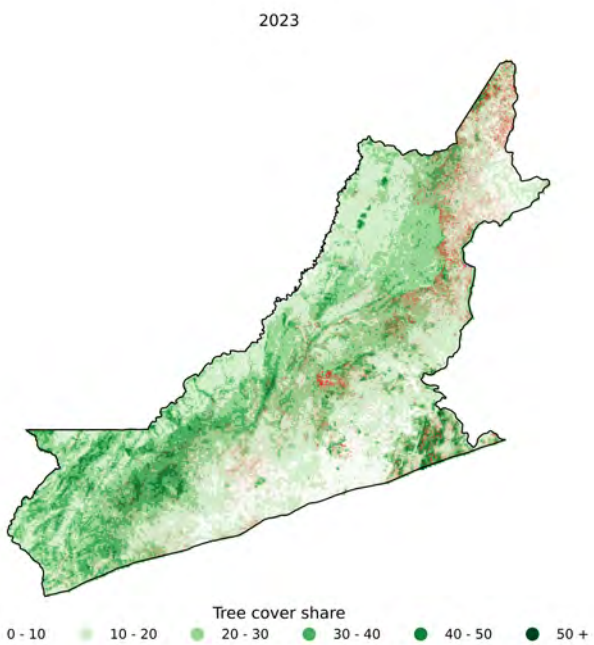
**(b)** Mambwe District

*Note: This map illustrates the overlapping of geographical layers in Zambia. Black lines delineate the country division according to chiefdom boundaries. The green layer represents the Natural Parks, the gray layer shows the Game Management Areas, and the red layer indicates the protected areas defined by the program. The hashed area indicates the Chiefdoms within the corridor aimed to be protected by the program. Figure 2 shows the Eastern province, and figure 2b shows Mambwe district.*

**Fig. 3.** Eastern Province baseline tree cover and tree cover loss in 2023



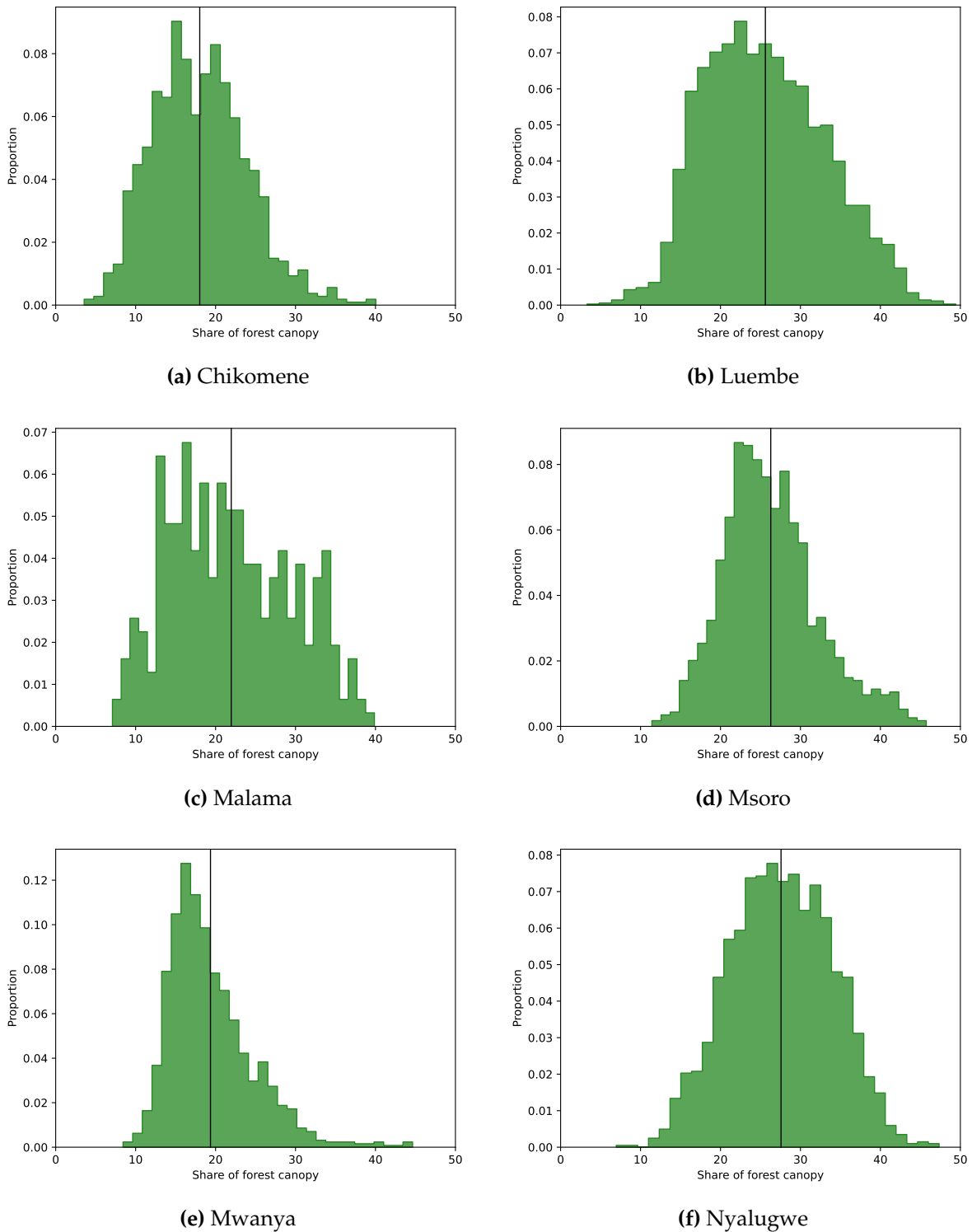
(a) Tree cover in 2000



(b) Cell tree cover loss in 2023

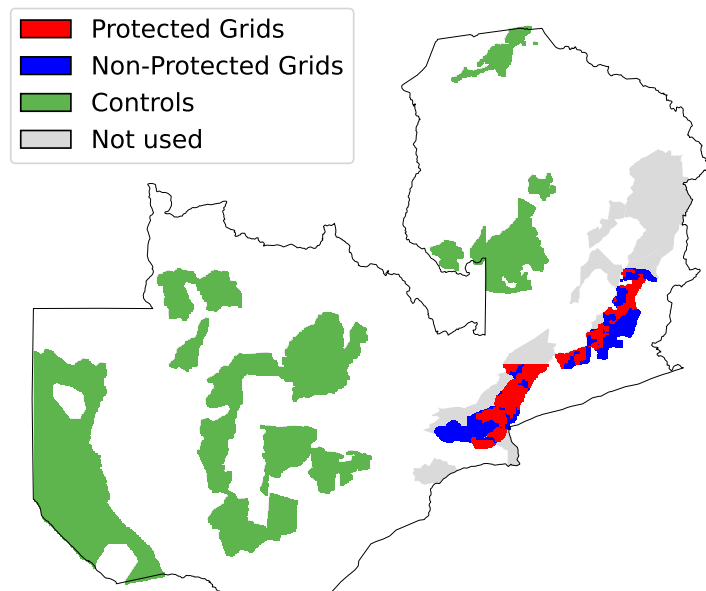
Note: The maps plot tree cover in 2000 and tree cover loss in 2023, using 30m x 30m Hansen cells. Figure 3a maps the tree cover in 2000 for each cell, and Figure 3b highlights the deforested cells in 2023, shown in red.

**Fig. 4.** Chiefdom distribution of 0.1-degree cell share of tree cover

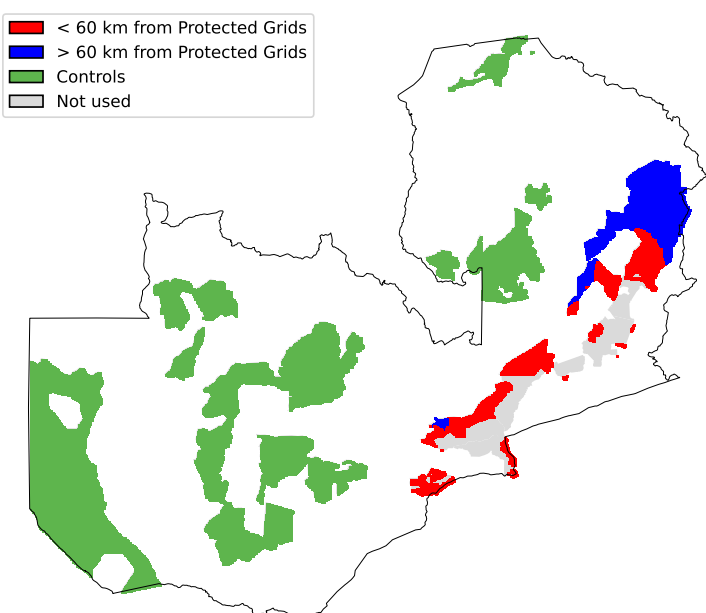


*Note: This Figure presents the 0.1 degree cell share of tree cover distributions of Chiefdoms surveyed by USAID in 2015 and 2024. The x-axis corresponds to the cell share of forest canopy, i.e., the proportion of the cell which is populated by crowns of trees. The y-axis corresponds to the proportion of cells within a share of canopy bin.*

**Fig. 5.** Spatial Distribution of Analytical Samples for Contracted and Non-Contracted Chiefdoms



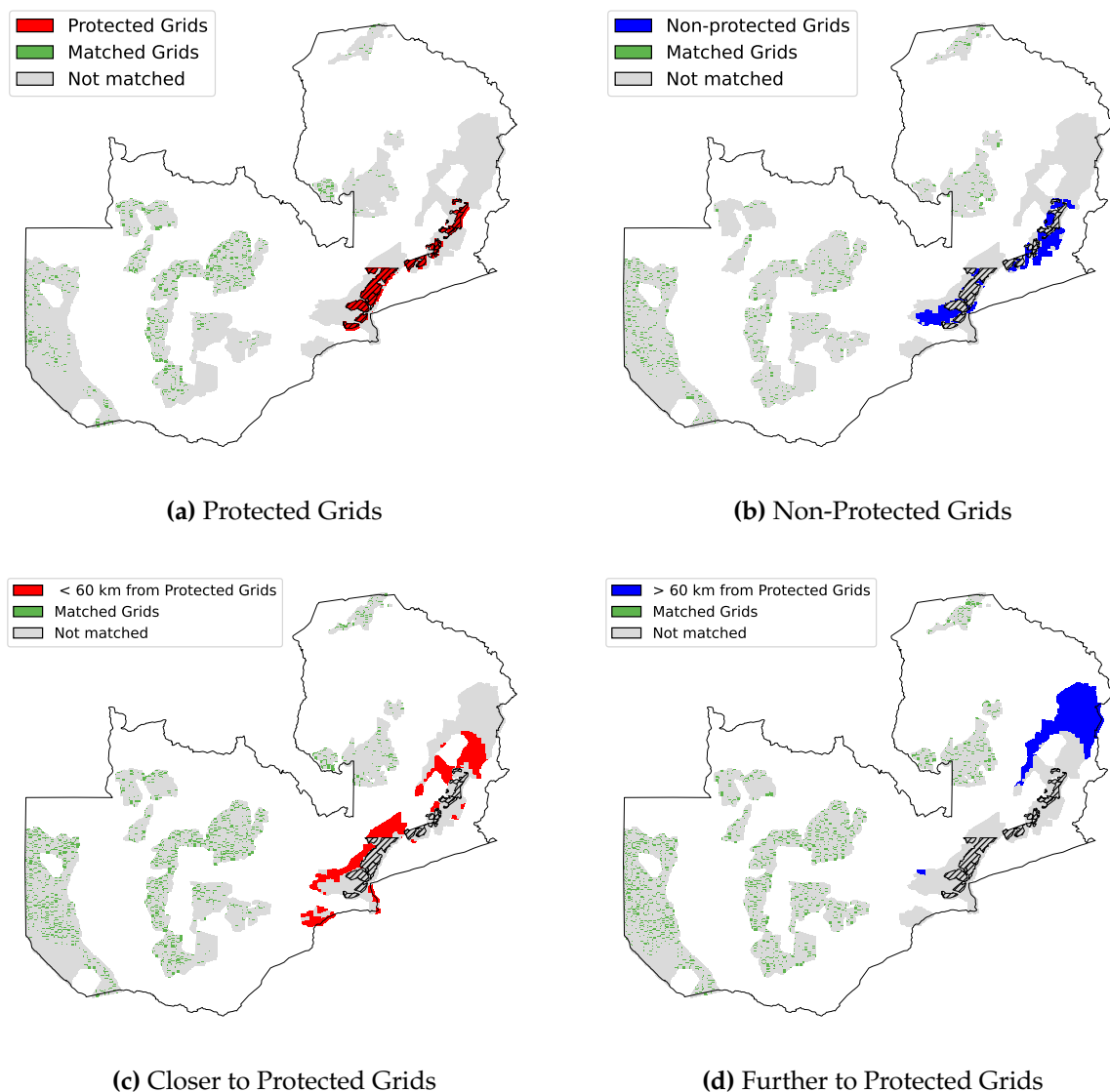
(a) Contracted Chiefdom



(b) Non-Contracted Chiefdom

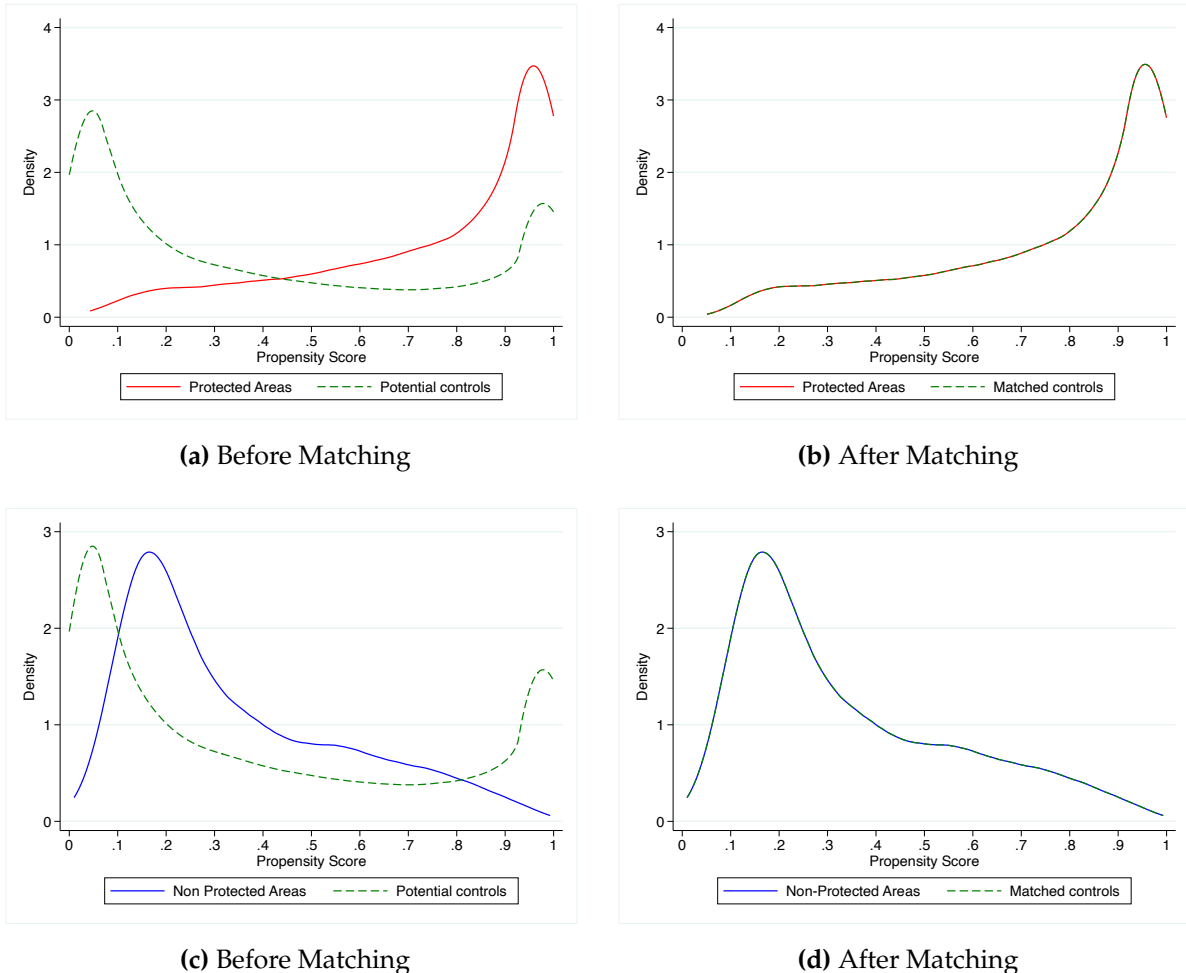
Note: This figure shows the geographic distribution of the 0.1-degree grids used in the analysis for two groups: Contracted Chiefdoms and Non-Contracted. Figure (5a) shows Protected Grids in red, Non-Protected Grids in blue, and controls in green. Figure (5b) shows Grids < 60 km from Protected Areas in red, > 60 km from Protected Areas in blue, and controls in green.

**Fig. 6. Spatial Distribution of Matched Samples**



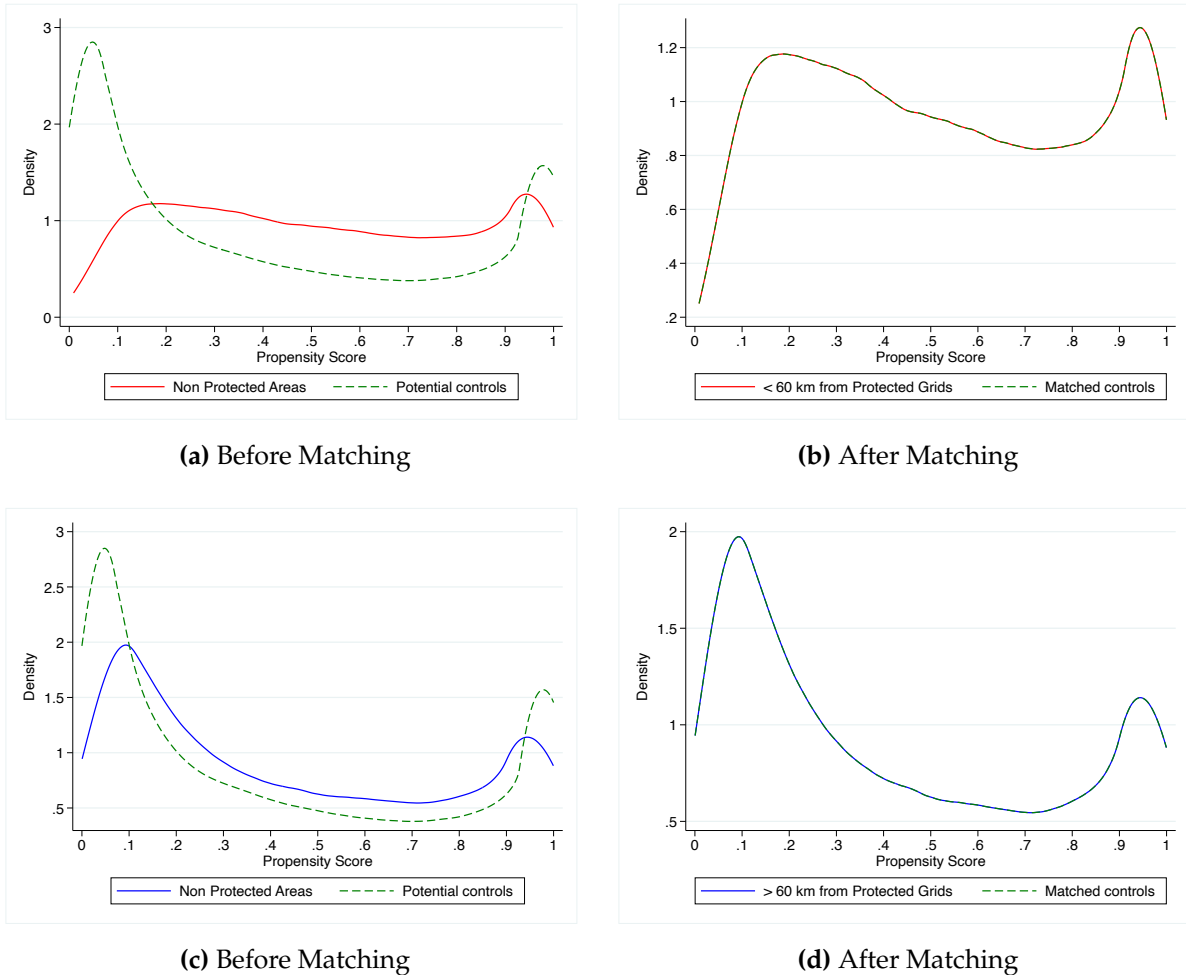
Note: This figure shows the geographic distribution of the 0.1-degree grids used in the matched analysis for four Grid groups: Protected (6a), Non-Protected(6b), < 60 km from Protected Grids(6c), and 60 km from Protected Grids (6d). The maps illustrate treatment groups (red and blue) and matched controls (green).

**Fig. 7.** Propensity Score distributions overlap for Contracted Chiefdoms



*Note: This figure shows the distribution of estimated propensity scores for treatment and potential control groups before and after matching for grids within Contracted Chiefdoms. Panels 7a and 7b show the overlap for protected areas versus matched controls, while panels 7c and 7d show the overlap for non-protected areas versus matched controls. Better overlap after matching in both comparisons suggests that the matching procedure improved balance between treated and control units.*

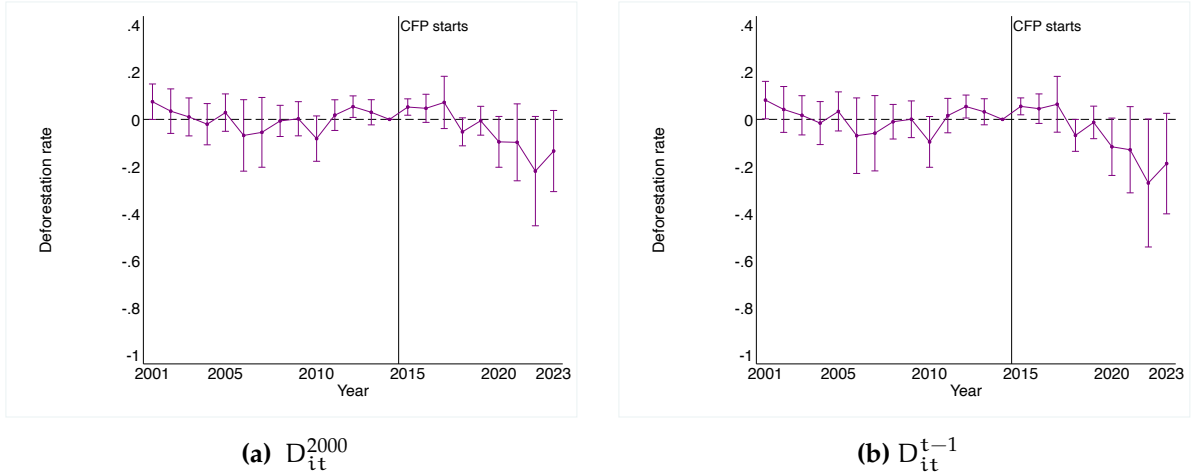
**Fig. 8.** Propensity Score distributions overlap for Non-Contracted Chiefdoms



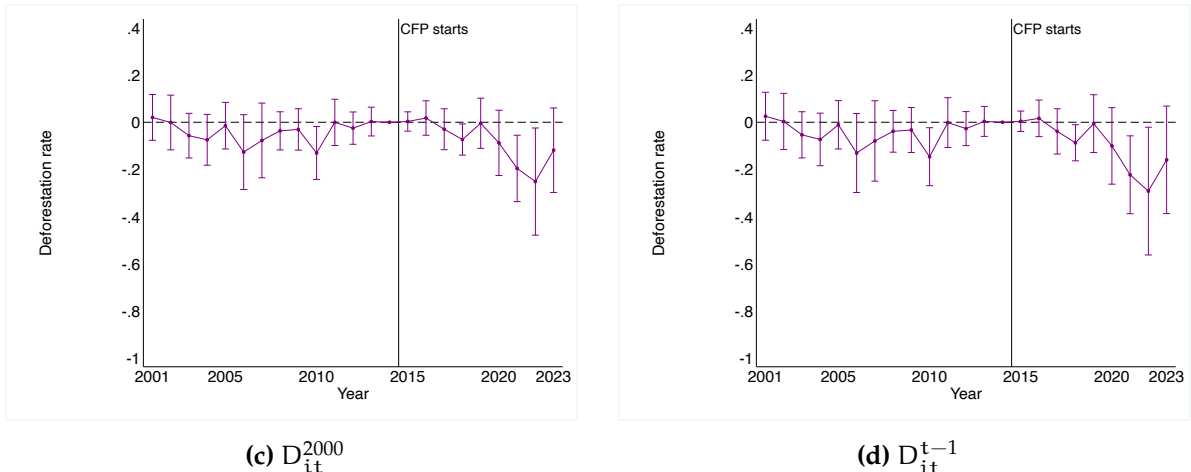
*Note: This figure shows the distribution of estimated propensity scores for treatment and potential control groups before and after matching for grids within Non-Contracted Chiefdoms. Panels 8a and 8b show the overlap for grids  $< 60 \text{ km}$  from protected areas versus matched controls, while panels 8c and 8d show the overlap for grid  $\geq 60 \text{ km}$  from protected areas versus matched controls.*

**Fig. 9.** Event study estimates for Contracted Chiefdoms

### Contracted Chiefdoms

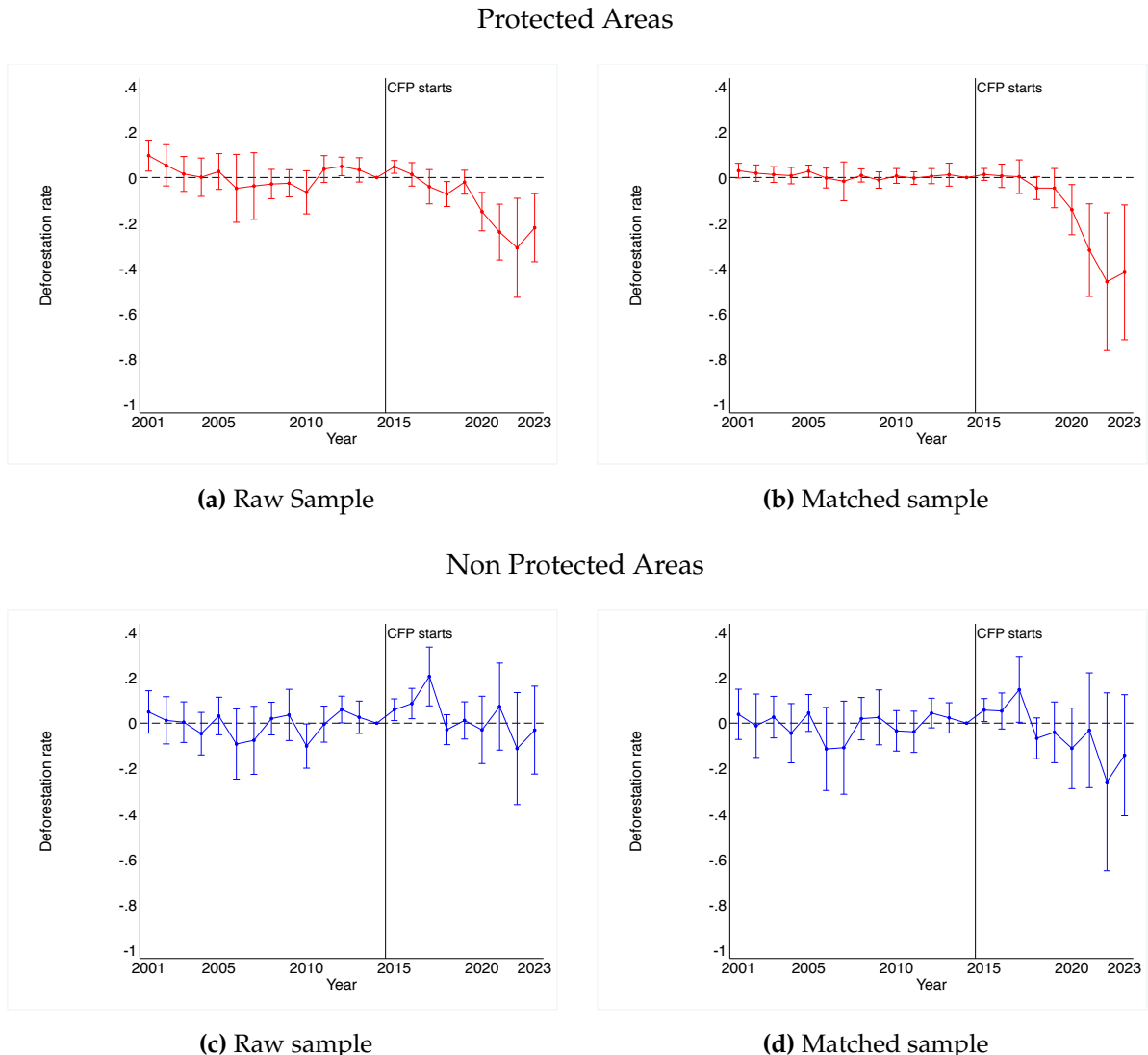


### Non-Contracted Chiefdoms



*Note:* This figure presents event study estimates of the impact of the Community Forest Program on annual deforestation rates for Contracted and Non-Contracted Chiefdoms. Panels 9a and 9b show the estimates for the Contracted Chiefdom's annual deforestation rate relative to the forest stock in 2000 and in the previous year, respectively. Panels 9c and 9d display the corresponding estimates for non-Contracted Chiefdoms. The vertical line indicates the beginning of the intervention. Each point represents the estimated difference in annual deforestation rate relative to the year before the intervention, with 95% confidence intervals.

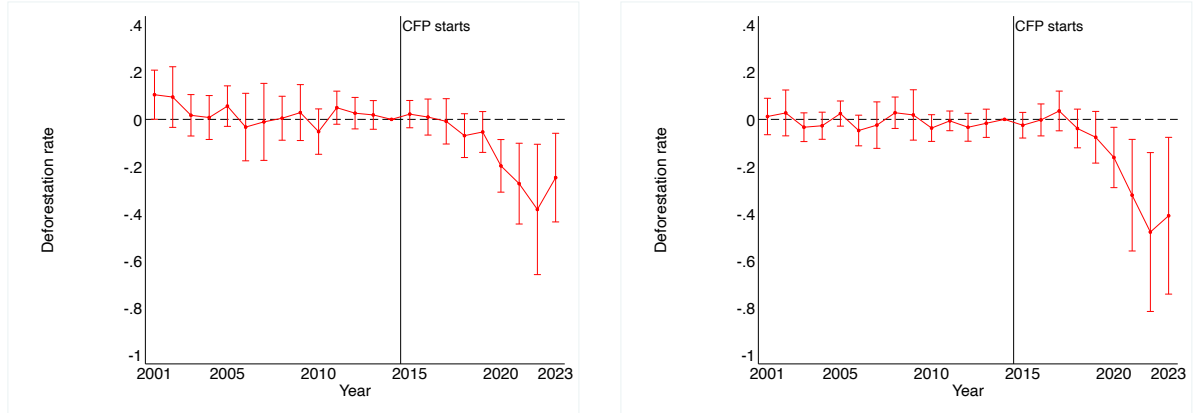
**Fig. 10.** Event study estimates for Contracted Chiefdoms ( $D_{it}^{2000}$ )



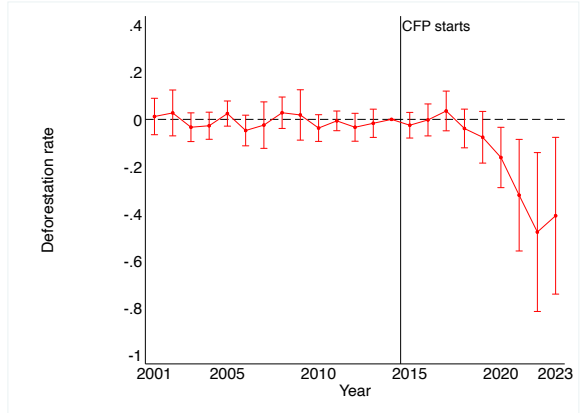
Note: This figure presents event study estimates of the impact of the Community Forest Program on annual deforestation rates relative to the forest stock in 2000 for Protected and Non-Protected Grids. Panels 10a and 10b show the estimates for Protected Grids using the raw and matched samples, respectively. Panels 10c and 10d display the corresponding estimates for Non-Protected Grids. The vertical line indicates the beginning of the intervention. Each point represents the estimated difference in annual deforestation rate relative to the year before the intervention, with 95% confidence intervals.

**Fig. 11.** Event study estimates for Non Contracted Chiefdoms ( $D_{it}^{2000}$ )

$< 60 \text{ km from PAs}$

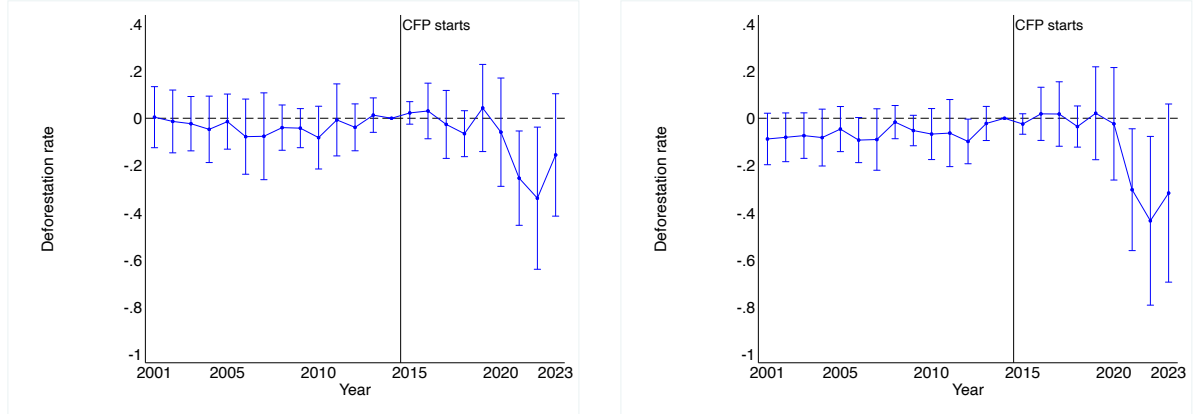


(a) Raw sample

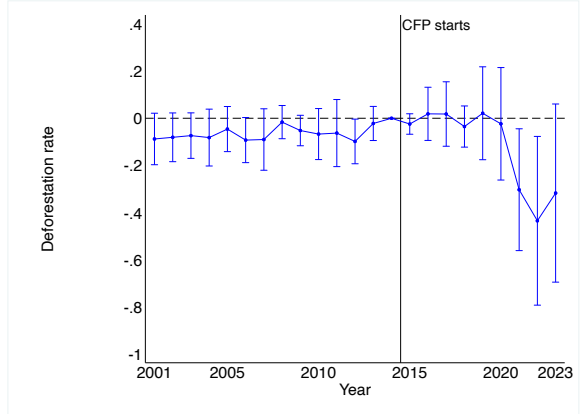


(b) Match sample

$\geq 60 \text{ km from PAs}$



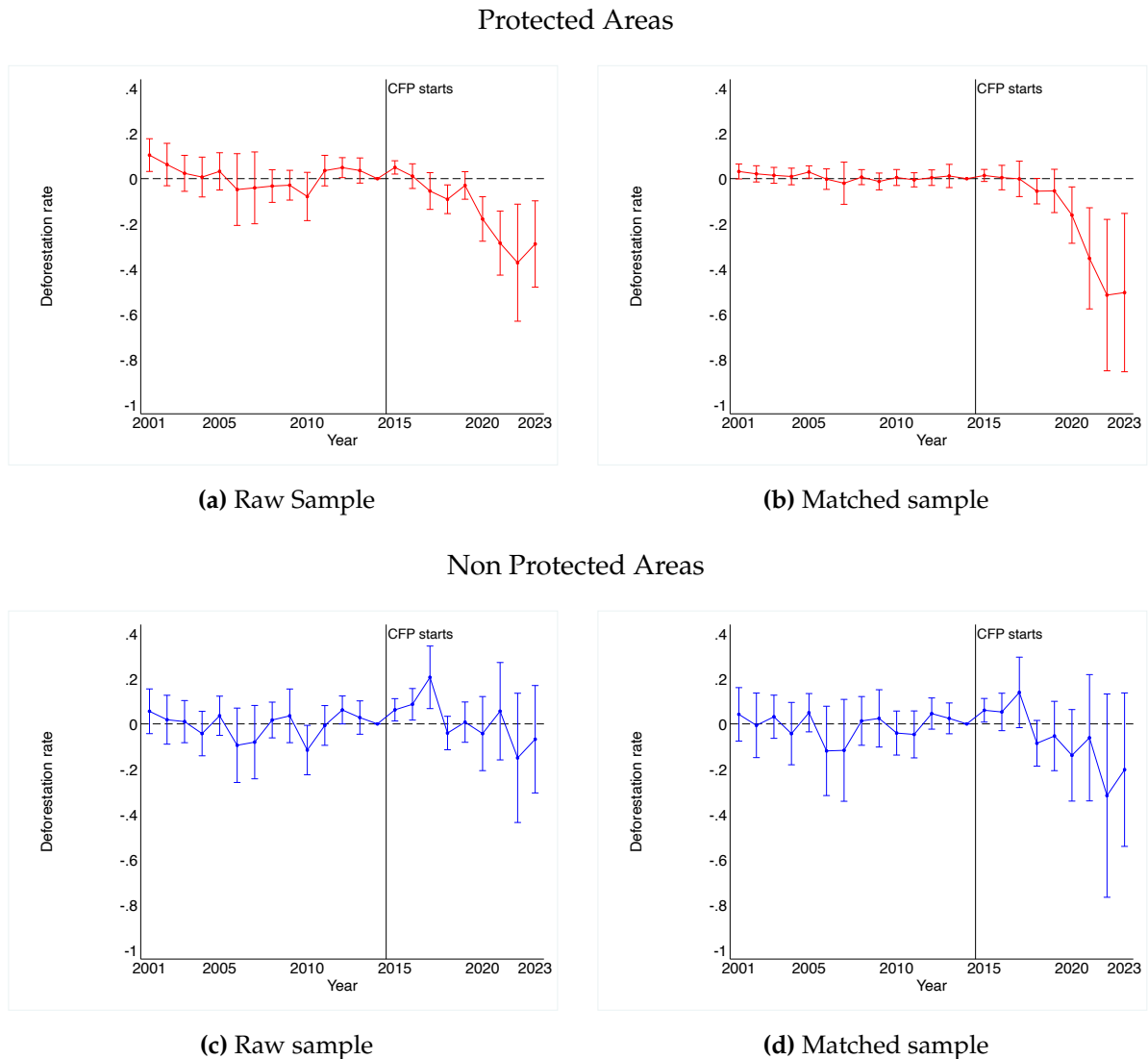
(c) Raw sample



(d) Match sample

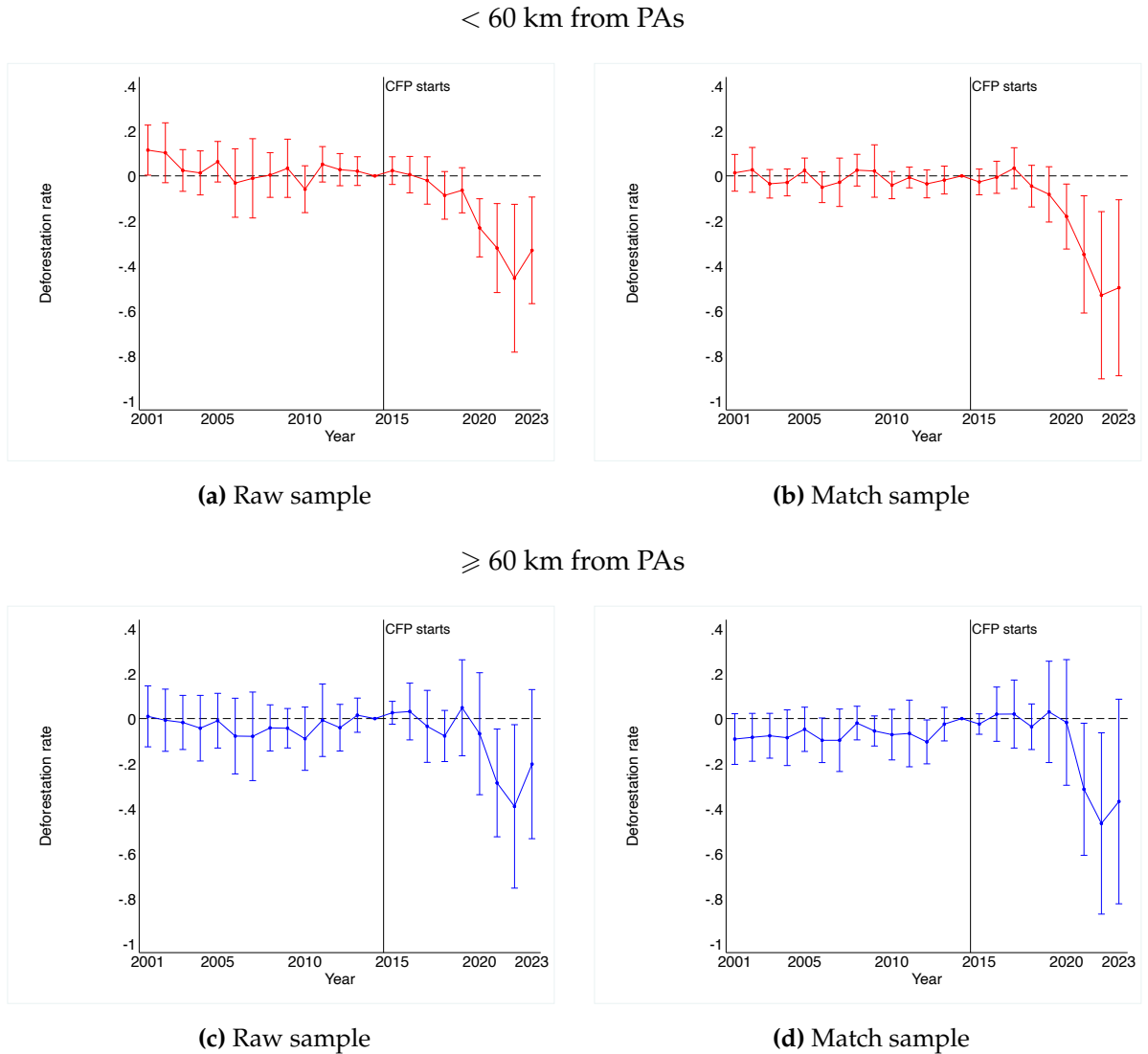
Note: This figure presents event study estimates of the impact of the Community Forest Program on annual deforestation rates relative to the forest stock in 2000 for Grids and  $\geq 60 \text{ km from Protected Areas}$ . Panels 11a and 11b show the estimates for Grids  $< 60 \text{ km from Protected Areas}$  using the raw and matched samples, respectively. Panels 11c and 11d display the corresponding estimates for Grids  $\geq 60 \text{ km from Protected Areas}$ . The vertical line indicates the beginning of the intervention. Each point represents the estimated difference in annual deforestation rate relative to the year before the intervention, with 95% confidence intervals.

**Fig. 12.** Event study estimates for Contracted Chiefdoms ( $D_{it}^{t-1}$ )



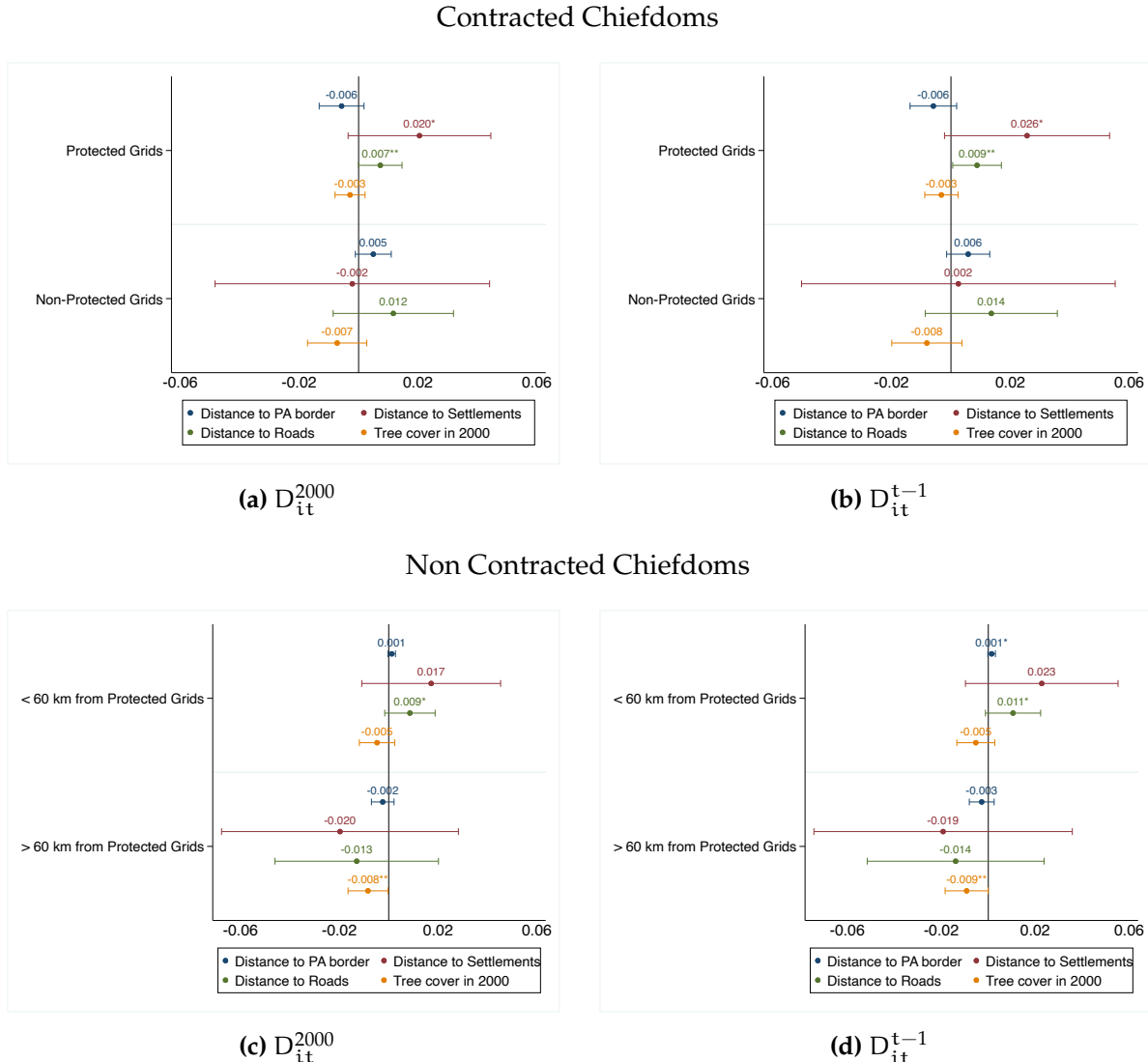
Note: This figure presents event study estimates of the impact of the Community Forest Program on annual deforestation rates relative to the forest stock in the previous year for Protected and Non-Protected Grids. Panels 12a and 12b show the estimates for Protected Grids using the raw and matched samples, respectively. Panels 12c and 12d display the corresponding estimates for Non-Protected Grids. The vertical line indicates the beginning of the intervention. Each point represents the estimated difference in annual deforestation rate relative to the year before the intervention, with 95% confidence intervals.

**Fig. 13.** Event study estimates for Non Contracted Chiefdoms ( $D_{it}^{t-1}$ )



Note: This figure presents event study estimates of the impact of the Community Forest Program on annual deforestation rates relative to the stock of forest in the previous year for Grids  $<$  and  $\geq 60 \text{ km from Protected Areas}$ . Panels 13a and 13b show the estimates for Grids  $< 60 \text{ km from Protected Areas}$  using the raw and matched samples, respectively. Panels 13c and 13d display the corresponding estimates for Grids  $\geq 60 \text{ km from Protected Areas}$ . The vertical line indicates the beginning of the intervention. Each point represents the estimated difference in annual deforestation rate relative to the year before the intervention, with 95% confidence intervals.

**Fig. 14.** Heterogeneous effects estimates for Contracted and Non-Contracted Chiefdoms



Note: This figure presents the estimates for heterogeneous effects for Contracted Chiefdoms and Non-Contracted Chiefdoms. Panel 14a and 14b present the estimates for Grids within Contracted Chiefdoms using annual deforestation rate relative to forest stock in 2000 and previous years, respectively. Panel 14c and 14d present the estimates for Grids within Non-Contracted Chiefdoms using annual deforestation rate relative to forest stock in 2000 and previous years, respectively. The heterogeneity analysis uses the Grids' distance in km from the Protected Areas border (blue), to Settlements (red), roads (green), and relative to the mean Grid share of tree cover in 2000. Each point represents the estimated difference in annual deforestation rate from an additional unit increase in any of the heterogeneity dimensions. The estimates have 95% confidence intervals.

Table 1: Corridor GMAs summary statistics by group

	Controls	Not Contracted	Contracted		
			PA and NPA	PA	NPA
Cell canopy share in 2000 (%)	22.425 (16.78)	24.645 (8.93)	22.875 (6.87)	23.486 (7.28)	22.200 (6.33)
Tree cover loss in m <sup>2</sup> (2001-2014)	5688.723 (19423.26)	4407.218 (14648.22)	2780.311 (9463.16)	789.580 (3156.94)	4979.649 (12972.01)
Average annual tree cover loss in m <sup>2</sup>	406.337 (1387.38)	314.801 (1046.30)	198.594 (675.94)	56.399 (225.50)	355.689 (926.57)
Average annual rate of tree loss in % (2001-2014)	0.123 (0.34)	0.068 (0.22)	0.041 (0.13)	0.011 (0.05)	0.074 (0.18)
Altitude (m)	1108.745 (85.77)	809.447 (232.71)	707.903 (149.39)	688.598 (132.69)	729.232 (163.28)
Maize Potential Yield (kg/acre)	3173.598 (173.42)	2979.733 (137.97)	3089.779 (96.44)	3100.313 (81.17)	3078.140 (109.73)
Distance to human settlements (km)	3.679 (4.41)	3.794 (3.30)	3.687 (3.19)	5.373 (3.23)	1.824 (1.80)
Distance to roads (km)	6.642 (6.89)	4.802 (4.66)	6.969 (5.86)	9.137 (6.19)	4.575 (4.35)
Distance to Electrical network (km)	70.259 (42.82)	46.762 (30.77)	65.218 (38.42)	75.021 (37.65)	54.388 (36.30)
Observations	98742	29902	15426	8097	7329

Note: This table presents summary statistics for Corridor Game Management Areas (GMAs). The GMAs observations are divided into Not-Contracted Chiefdoms and Contracted Chiefdoms. Contracted Chiefdoms are split into Protected Areas (PA) and Non-Protected Areas (NPA). The table presents the mean value for 1km × 1km blocks within each group. Standard errors are presented in parentheses.

Table 2: Estimates of CFP's impact on Contracted Chiefdom's Annual Deforestation rate

	Raw sample		Matched sample	
	$D_{it}^{2000}$	$D_{it}^{t-1}$	$D_{it}^{2000}$	$D_{it}^{t-1}$
Contracted Chiefdom	-0.050 (0.062)	-0.071 (0.071)		
Contracted - Protected		-0.119** (0.056)	-0.146** (0.064)	-0.164*** (0.060)
Contracted - Not Protected		0.032 (0.065)	0.019 (0.074)	-0.035 (0.092)
R <sup>2</sup>	0.04	0.04	0.04	0.04
Observations	2,596,332	2,596,332	2,596,306	2,596,306
Chiefdom FE	Yes	Yes	Yes	Yes
Year FE	Yes	Yes	Yes	Yes

Note: This table shows the estimates of the Community Forest Community on Contracted Chiefdoms Grids, Protected Areas, and Non-Protected Areas. The dependent variable in all specifications is the annual deforestation rate. Columns (1) to (4) present regression results based on the raw sample, while columns (5) to (8) use matched samples. For each sample, the first two columns report estimates using the annual deforestation rate calculated relative to the baseline forest stock in the year 2000, whereas the latter two columns use the annual deforestation rate relative to forest stock in the previous year. Standard deviations are reported in parentheses. Standard errors are clustered at the chiefdom level. Standard deviations are reported in parentheses, and errors are clustered at the chiefdom level. \*, \*\*, \*\*\* denote statistical significance at the 10%, 5%, and 1% level, respectively.

Table 3: Estimates of CFP's impact on Non-Contracted Chiefdom's Annual Deforestation rate

	Raw sample				Matched sample			
	D <sub>it</sub> <sup>2000</sup>	D <sub>it</sub> <sup>t-1</sup>	D <sub>it</sub> <sup>2000</sup>	D <sub>it</sub> <sup>t-1</sup>				
Non Contracted Chiefdom	-0.043 (0.076)	-0.058 (0.087)						
< 60 km from PAs		-0.102* (0.060)	-0.128* (0.069)	-0.157** (0.072)		-0.186** (0.081)		
≥ 60 km from PAs		0.012 (0.110)	0.006 (0.126)		-0.029 (0.117)		-0.040 (0.134)	
R <sup>2</sup>	0.04	0.04	0.04	0.04	0.04	0.05	0.04	0.05
Observations	2,868,238	2,868,238	2,868,212	2,868,212	611,662	656,696	611,662	656,696
Chiefdom FE	Yes	Yes	Yes	Yes	Yes	Yes	Yes	Yes
Year FE	Yes	Yes	Yes	Yes	Yes	Yes	Yes	Yes

Note: This table shows the estimates of the Community Forest Community on Grids within Non-Contracted Chiefdoms, < 60 Km from Protected Areas, and ≥ 60 Km from Protected Areas. The dependent variable in all specifications is the annual deforestation rate. Columns (1) to (4) present regression results based on the raw sample, while columns (5) to (8) use matched samples. For each sample, the first two columns report estimates using the annual deforestation rate calculated relative to the baseline forest stock in the year 2000, whereas the latter two columns use the annual deforestation rate relative to forest stock in the previous year. Standard deviations are reported in parentheses. Standard errors are clustered at the chiefdom level. Standard deviations are reported in parentheses, and errors are clustered at the chiefdom level. \*, \*\*, \*\*\* denote statistical significance at the 10%, 5%, and 1% level, respectively.

## References

- Abman, Ryan, and Clark Lundberg. 2024. "Contracting, Market Access and Deforestation." *Journal of Development Economics* 168 (May): 103269. <https://doi.org/10.1016/j.jdeveco.2024.103269>. <https://www.sciencedirect.com/science/article/pii/S030438782400018X>.
- Baland, Jean-Marie, Pranab Bardhan, Sanghamitra Das, and Dilip Mookherjee. 2010. "Forests to the People: Decentralization and Forest Degradation in the Indian Himalayas." *World Development* 38, no. 11 (November): 1642–1656. <https://doi.org/10.1016/j.worlddev.2010.03.007>. <https://www.sciencedirect.com/science/article/pii/S0305750X10000896>.
- Balboni, Clare, Aaron Berman, Robin Burgess, and Benjamin A. Olken. 2023. "The Economics of Tropical Deforestation." *Annual Review of Economics* 15, no. Volume 15, 2023 (September): 723–754. <https://doi.org/10.1146/annurev-economics-090622-024705>. <https://www.annualreviews.org/content/journals/10.1146/annurev-economics-090622-024705>.
- Baldwin, Kate. 2013. "Why Vote with the Chief? Political Connections and Public Goods Provision in Zambia." *American Journal of Political Science* 57, no. 4 (October): 794–809. <https://doi.org/10.1111/ajps.12023>. <https://onlinelibrary.wiley.com/doi/10.1111/ajps.12023>.
- . 2015. *The Paradox of Traditional Chiefs in Democratic Africa*. Cambridge Studies in Comparative Politics. Cambridge: Cambridge University Press. <https://doi.org/10.1017/CBO9781316422335>. <https://www.cambridge.org/core/books/paradox-of-traditional-chiefs-in-democratic-africa/A0A5A0A8B513F792F501C82AF5935457>.
- Baragwanath, Kathryn, and Ella Bayi. 2020. "Collective Property Rights Reduce Deforestation in the Brazilian Amazon." *Proceedings of the National Academy of Sciences* 117, no. 34 (August): 20495–20502. <https://doi.org/10.1073/pnas.1917874117>. <https://www.pnas.org/doi/full/10.1073/pnas.1917874117>.
- Bellemare, Marc F., and Casey J. Wichman. 2020. "Elasticities and the Inverse Hyperbolic Sine Transformation." *Oxford Bulletin of Economics and Statistics* 82 (1): 50–61. <https://doi.org/10.1111/obes.12325>. <https://onlinelibrary.wiley.com/doi/abs/10.1111/obes.12325>.
- Burgess, Robin, Matthew Hansen, Benjamin A. Olken, Peter Potapov, and Stefanie Sieber. 2012. "The Political Economy of Deforestation in the Tropics\*." *The Quarterly Journal of Economics* 127, no. 4 (November): 1707–1754. <https://doi.org/10.1093/qje/qjs034>. <https://doi.org/10.1093/qje/qjs034>.
- Cattaneo, Matias D., Nicolás Idrobo, and Rocío Titiunik. 2019. "A Practical Introduction to Regression Discontinuity Designs: Foundations." *Elements in Quantitative and Computational Methods for the Social Sciences* (November). <https://doi.org/10.1017/9781108684606>. <https://www.cambridge.org/core/elements/practical-introduction-to-regression-discontinuity-designs/F04907129D5C1B823E3DB19C31CAB905>.
- Chen, Jiafeng, and Jonathan Roth. 2024. "Logs with Zeros? Some Problems and Solutions\*." *The Quarterly Journal of Economics* 139, no. 2 (May): 891–936. <https://doi.org/10.1093/qje/qjad054>. <https://doi.org/10.1093/qje/qjad054>.
- Cisneros, Elías, Jan Börner, Stefano Pagiola, and Sven Wunder. 2022. "Impacts of Conservation Incentives in Protected Areas: The Case of Bolsa Floresta, Brazil." *Journal of Environmental Economics and Management* 111 (January): 102572. <https://doi.org/10.1016/j.jeem.2021.102572>. <https://www.sciencedirect.com/science/article/pii/S0095069621001200>.

- Cisneros, Elías, and Krisztina Kis-Katos. 2022. "Unintended Consequences of Anti-Corruption Strategies." (Rochester, NY) (March). <https://doi.org/10.2139/ssrn.3899498>. <https://papers.ssrn.com/abstract=3899498>.
- Correa, Juliano, Elías Cisneros, Jan Börner, Alexander Pfaff, Marcelo Costa, and Raoni Rajão. 2020. "Evaluating REDD+ at Subnational Level: Amazon Fund Impacts in Alta Floresta, Brazil." *Forest Policy and Economics* 116 (July): 102178. <https://doi.org/10.1016/j.forepol.2020.102178>. <https://www.sciencedirect.com/science/article/pii/S1389934119301170>.
- Correia, Sergio, Paulo Guimarães, and Thomas Zylkin. 2019. *Ppmlhdfe: Fast Poisson Estimation with High-Dimensional Fixed Effects*, August. <https://doi.org/10.48550/arXiv.1903.01690>. <http://arxiv.org/abs/1903.01690>.
- Giudice, Renzo, Jan Börner, Sven Wunder, and Elias Cisneros. 2019. "Selection Biases and Spillovers from Collective Conservation Incentives in the Peruvian Amazon." *Environmental Research Letters* 14, no. 4 (April): 045004. <https://doi.org/10.1088/1748-9326/aafc83>. <https://dx.doi.org/10.1088/1748-9326/aafc83>.
- Gollin, Douglas, and Julien Wolfersberger. 2024. "Agricultural Trade and Deforestation: The Role of New Roads."
- Gourieroux, Christian, Alain Monfort, and Alain Trognon. 1984. "Pseudo Maximum Likelihood Methods: Applications to Poisson Models." *Econometrica* 52 (3): 701–20. [https://econpapers.repec.org/article/ecmemetrp/v\\_3a52\\_3ay\\_3a1984\\_3ai\\_3a3\\_3ap\\_3a701-20.htm](https://econpapers.repec.org/article/ecmemetrp/v_3a52_3ay_3a1984_3ai_3a3_3ap_3a701-20.htm).
- Gulzar, Saad, Apoorva Lal, and Benjamin Pasquale. 2024. "Representation and Forest Conservation: Evidence from India's Scheduled Areas." *American Political Science Review* 118, no. 2 (May): 764–783. <https://doi.org/10.1017/S0003055423000758>. <https://www.cambridge.org/core/journals/american-political-science-review/article/representation-and-forest-conservation-evidence-from-indias-scheduled-areas/BF8BB4821C97E6E67E682D71345DA0FE>.
- Hansen, James, Makiko Sato, Gary Russell, and Pushker Kharecha. 2013. "Climate Sensitivity, Sea Level and Atmospheric Carbon Dioxide." *Philosophical Transactions of the Royal Society A: Mathematical, Physical and Engineering Sciences* 371, no. 2001 (October): 20120294. <https://doi.org/10.1098/rsta.2012.0294>. <https://royalsocietypublishing.org/doi/10.1098/rsta.2012.0294>.
- Jack, B. Kelsey, Seema Jayachandran, Namrata Kala, and Rohini Pande. 2022. *Money (Not) to Burn: Payments for Ecosystem Services to Reduce Crop Residue Burning*. Working Paper, November. <https://doi.org/10.3386/w30690>. <https://www.nber.org/papers/w30690>.
- Jayachandran, Seema. 2022. "The Inherent Trade-Off Between the Environmental and Anti-Poverty Goals of Payments for Ecosystem Services," Working Paper Series (April). <https://doi.org/10.3386/w29954>. <https://www.nber.org/papers/w29954>.
- Malan, Mandy, Rachel Carmenta, Elisabeth Gsottbauer, Paul Hofman, Andreas Kontoleon, Tom Swinfield, and Maarten Voors. 2024. "Evaluating the Impacts of a Large-Scale Voluntary REDD+ Project in Sierra Leone." *Nature Sustainability* 7, no. 2 (February): 120–129. <https://doi.org/10.1038/s41893-023-01256-9>. <https://www.nature.com/articles/s41893-023-01256-9>.
- Silva, J. M. C. Santos, and Silvana Tenreyro. 2006. "The Log of Gravity." *The Review of Economics and Statistics* 88, no. 4 (November): 641–658. <https://doi.org/10.1162/rest.88.4.641>. <https://doi.org/10.1162/rest.88.4.641>.

- Sims, Katharine R. E. 2010. "Conservation and Development: Evidence from Thai Protected Areas." *Journal of Environmental Economics and Management* 60, no. 2 (September): 94–114. <https://doi.org/10.1016/j.jeem.2010.05.003>. <https://www.sciencedirect.com/science/article/pii/S0095069610000586>.
- Sze, Jocelyne S., L. Roman Carrasco, Dylan Childs, and David P. Edwards. 2022. "Reduced Deforestation and Degradation in Indigenous Lands Pan-Tropically." *Nature Sustainability* 5, no. 2 (February): 123–130. <https://doi.org/10.1038/s41893-021-00815-2>. <https://www.nature.com/articles/s41893-021-00815-2>.
- USAID. 2016. *Report on Baseline Findings, Community Forest Management Program*. Technical Report. USAID.
- . 2019. *Community Forests Program Final Report 2014 - 2019*. Technical Report. USAID.
- Watson, Charlene, Liane Schalatek, and Aurélien Evéquoz. 2020. "Climate Finance Thematic Briefing: REDD+ Finance."
- Wooldridge, Jeffrey M. 2023. "Simple Approaches to Nonlinear Difference-in-Differences with Panel Data." *The Econometrics Journal* 26, no. 3 (September): C31–C66. <https://doi.org/10.1093/ectj/utad016>. <https://academic.oup.com/ectj/article/26/3/C31/7250479>.

# ONLINE APPENDIX

## Strategic Environment:

### Conservation Policies Effectiveness and Strategic Behavior

## A Additional Data Details (Online)

### A.1 Tree cover data

To measure tree cover and tree cover loss, I used the [Global Forest Change \(GFC\)](#) (Hansen et al. 2013) from the University of Maryland. This dataset was created based on a set of Landsat images since 2000, providing yearly layers on tree cover change for the all globe. This dataset is publicly available for download and can be used in the Google Engine platform for visualizations and data processing.

The dataset has a spatial resolution of 1 arc-second per pixel or approximately 30 meters per pixel at the equator. We use two layers of tree cover information. First, I used the tree canopy cover for the year 2000. This defines the share of forest canopy for each 30x30m grid, defining a tree as any vegetation taller than 5m in height. The information is the percentage per grid cell of forest canopy, ranging from 0-100. This layer is my baseline data and there are no year updates on the forest canopy share per grid, which is a caveat of using the GFC data. The second layer measures tree cover loss defined as a stand-replacement disturbance or a change from a forest to a non-forest state at the grid level. The cell level information ranges from 0 to 20, where 0 represents no loss and 1 to 23 represents loss detected primarily in the years 2001-2023, respectively.

In addition to these layers, the GFC has 4 more layers. There is a layer of forest cover gain from 2000- to 2012, which is defined as the inverse of loss, or a non-forest-to-forest change entirely within the period. The information is encoded as 1 (gain) or 0 (no gain). Another available is the data mask for cells where 0 represents areas with no data, 1 for mapped land surface, and 2 for persistent water bodies based on 2000 to 2012. The last two layers are the Circa year 2000 Landsat 7 cloud-free image composite and the Circa year 2023 Landsat cloud-free image composite. The first contains reference multispectral imagery from the first available year, typically 2000. The list contains reference multispectral imagery from the last available year, typically 2023.

The dataset is downloaded by 10x10 degree combinations through the website. To pro-

cess the dataset for my location of interest, I have determined a latitude-longitude box and filtered the 10x10 degree datasets. After filtering the layers, I overlapped location boundaries (chiefdom, protected areas, and village areas) to aggregate 30x30m to the 0.1-degree cell level combinations.

## A.2 Fires data

To measure the fire events I will use the [Fire Information for Resource Management System \(FIRMS\)](#) from NASA. This dataset provides Near Real-Time (NRT) active fire data using images from the Moderate Resolution Imaging Spectroradiometer (MODIS) and Visible Infrared Imaging Radiometer Suite (VIIRS). The NRT data is available within 3 hours of satellite observations, except the US and Canada which have real-time data. The resolution is 375m and the data is available since 20 January 2012. This dataset is publicly available for the all globe and can be downloaded through the NASA Earthdata API.

Each 375m pixel has attributes on fire outcomes and technical information. The centroid of the 375m pixel is informed by latitude and longitude coordinates. To measure fire intensity, the dataset informs two scales of temperature in Kelvin reflected by channel brightness, Brightness temperature I-4 and Brightness temperature I-5. The information related to the timing of the event is the date, time, day, or night category. Regarding the confidence of the measure, there are three groups: Low, Nominal, and High confidence. This is determined by the fire intensity and sun glint. Low-confidence detection is typically linked to regions affected by Sun glint and has lower relative temperature anomalies (less than 15 K) in the mid-infrared channel I4. Fire Radiative Power (FRP) is another measurement of fire intensity, that is based on a hybrid approach combining 375 and 750 m data. Nominal-confidence detection is free from potential Sun glint contamination during the day and exhibits strong temperature anomalies (greater than 15 K) in either day or nighttime data. High-confidence detections are associated with saturated pixels, whether during the day or at night. More technical information includes the satellite source of observation, which could be the Suomi National Polar-orbiting Partnership (Suomi NPP), NOAA-20 (formally JPSS-1), and NOAA-21. Another source of technical information is the version of the data.

### A.3 Protected areas

The protected areas information used in the paper comes from the Planet protected data on protected areas and other effective area-based conservation measures (OECMs). This dataset contains the most complete and updated information on terrestrial and marine protected areas around the globe. The database contains shapefiles that inform multiple characteristics of these areas, such as location, type of protected area, ownership, forest management plan existence, and other characteristics.

An important information concerning these areas is the designation, which includes National Parks, Game Management Areas (GMAs), and Forest reserves. This is relevant to know as the rules relative to forest usage differ conditional on the designation type. For instance, Forest reserves do not have strict rules relative to forest usage as National Parks are strictly monitored and prohibit activities that can harm its biodiversity, and human settlements. The GMAs in Zambia are more flexible in terms of the rules, allowing Human settlements, and focus on rules for sustainable hunting in the area. According to the dataset, Zambia contains 20 National parks, 36 GMAs, and 464 Forest reserves.

### A.4 Zambia Rural Agricultural Livelihoods Survey (RALS)

I use the Zambia Rural Agricultural Livelihoods Survey (RALS), which provides comprehensive information on rural households across Zambia. This dataset is available under request and confidentiality agreement with the Indaba Agricultural Policy Research Institute (IAPRI).

The survey was conducted in 2012, 2015, and 2019 and serves as an important tool for understanding the dynamics of rural livelihoods, agricultural production, and rural development challenges in Zambia. RALS is a partnership between the Indaba Agricultural Policy Research Institute (IAPRI), the Central Statistical Office of Zambia, and the Ministry of Agriculture.

The sample of the study includes small and medium farmers, i.e. cultivating less than 20 Ha, and follows the Zambia 2010 Census sample. The dataset has 17 sections in 2019 and includes detailed data on agricultural practices, household demographics, livestock ownership, and economic activities. This dataset covers multiple dimensions of rural livelihoods, such as crop production, income sources, and access to essential services like credit and extension services. The survey's rich demographic and economic data, combined with its geographic

coordinates on household locations, allows it to map and construct geographical indicators.

### A.5 GRID3 Settlement Mapping

The GRID3 Settlement Mapping for Zambia provides detailed geospatial data identifying the location and extent of human settlements throughout the country. This mapping initiative combines satellite imagery with population data, helping to locate both urban and rural communities with high accuracy. The data captures the physical boundaries of settlements, which include residential areas, infrastructure, and other human-made structures. With the location of this settlement, it is possible to construct village-level outcomes by allocating cells to the closest settlement according to the data. This is done by creating Voronoi polygons.

### A.6 Cell aggregation

My main analysis relies on  $0.01 \times 0.01$  degrees cell grids, which corresponds to approximately  $1\text{km} \times 1\text{km}$ . I created these grids using the function `X` in Python, which rounds a given number to the Y border. I use this function for both the latitude and longitude coordinates of a particular cell and create a geoid. The geoid consists of the concatenation of the rounded latitude and longitude strings. For example, a cell located at -z and l will have the following geoid "`-z_l`".

After creating the  $0.01 \times 0.01$  geoids, I can aggregate cell values using aggregation functions. For example, I can compute the tree cover loss for each geoid in a particular year by using the sum aggregation function for the tree cover loss for smaller grids associated with this ID. For other variables, I take the mean, as tree cover in 2000.

### A.7 Geographical matching

To create multiple cell-level information I used geographical matching. I use an open-source package in Python called GeoPandas, which contains functions that perform geospatial operations. To match the multiple layers I use two methods I use the function `sjoin` which overlaps layers and matches them geographically. For example, using the shapefile of the Eastern province I can overlap with all the cells within the region and associate it with the province-level data.

## B Additional Method Details (Online)

In this section, I give more details about the empirical strategy used in the paper and additional methods that will be used to obtain more local effects, Regression discontinuity (RDD), and village-level effects (DiD).

**Issues with zero-valued based outcomes** Researchers use the inverse hyperbolic sine transformation applied to tree cover loss areas to deal with the occurrence of multiple zeros (Cisneros et al. 2022; Cisneros and Kis-Katos 2022; Abman and Lundberg 2024). The cyclical and gradual nature of deforestation activities generates observation-time combinations in which no tree cover loss will be observed, producing a considerable presence of zero values. The transformation not only deals with the zeros in the data but also enables to translation of the ATE coefficient to percentage changes in the outcome variable, which is very useful for interpretation purposes (Bellemare and Wichman 2020).

However, a recent paper by Chen and Roth (2024) suggests that estimations using log transformations may be sensitive unity scaling in the outcome variable. The paper shows that the extensive margin effects lead to issues in the percentage interpretation of ATE. This happens because the undefined percentage change from zero to a positive number is observed in the extensive margin effects of programs. In the case of tree cover loss, a cell that was not deforested before the policy implementation, and experienced tree cover loss after the policy does not have a well-defined percentage increase in tree cover loss. Additionally, the outcome unit ( $m^2$ ,  $km^2$ , ha) influences the distribution of the outcome variable, impacting the ATE estimation by changing the distribution dispersion. Because of that, the interpretation of the coefficients may be sensitive to the units of my outcome measure.

Chen and Roth (2024) propose three other estimators to use when using zero-valued outcomes, as they are not unit-dependent. To interpret the coefficient in percentage terms one can use Poisson regressions to recover the ATE in levels expressed as a percentage of the control mean (Gourieroux, Monfort, and Trognon 1984; Silva and Tenreyro 2006; Wooldridge 2023; Correia, Guimarães, and Zylkin 2019). This estimation is not scale-dependent and normalizes the ATE in levels. The parameter can be estimated using the following:

$$Y_{ict} = \exp(\theta_0 + \theta_{ATE\%} After_t \times Treated_c + \alpha_t + \delta_c) \epsilon_{ict} . \quad (B.1)$$

Where:

$$\theta_{ATE\%} = \frac{\mathbb{E}[Y(1) - Y(0)]}{\mathbb{E}[Y(0)]} . \quad (B.2)$$

To interpret this as a causal parameter, it is necessary to test for parallel trends which can be verified by using the Poisson version of the event study shown in Equation ??.

**REDD+ protected areas effects - Pure RDD** To estimate the impact of the protected areas initiated by the CFP program, I will use a Geographical Regression Discontinuity Design (RDD). Three main elements define this design: a score  $s$ , a cutoff  $c$ , and bandwidth choices (formalized below). The identification strategy relies on the fact that cells closer to the cutoff  $c$  are similar in observable and unobserved characteristics with the difference of the new protection boundaries. In my context, cells within the protected areas face a discrete change in the likelihood of being deforested after the conservation boundary implementation. This likelihood can be reflected by the score  $s$  of cells, which is a function of the distance to the protected areas' borders. Going further from the border of the PAs, the cells tend to be differentiated in multiple dimensions and decrease the score associated with the likelihood of being deforested. This highlights the importance of bandwidth  $h$  choice around the cutoff, as this influences the comparability of cells within the protected areas with contractual boundaries. The optimal bandwidth is estimated using non-parametric methods following Cattaneo, Idrobo, and Titiunik (2019) which minimizes the Mean Squared Error (MSE) influenced by the estimator bias-variance tradeoff.

To formalize the RDD, I define cell  $i$  and  $n_h$  as the total number of cells observed within the bandwidth  $h$ , where  $i = 1, 2, \dots, n_h$ . In addition,  $X_i = \{\text{lat}_i, \text{long}_i\}$  is the centroid of cell  $i$ . The cutoff  $c$  is the coordinates  $\{\text{lat}_c, \text{long}_c\}$  for the closest PA defined by the program. Treatment is defined by  $T_i \in \{0, 1\}$  where 1 indicates that cell  $i$  is treated, which happens when scoring  $s = 1$ . This includes cells for which the distance between cell  $i$  coordinates and the closest PA is positive ( $X_i - c \geq 0$ ) and  $c - h \leq X_i \leq c + h$ , where  $h$  corresponds to the optimal bandwidth. If the distance is negative ( $X_i - c \leq 0$ ) and  $c - h \leq X_i \leq c + h$ , the cell score is zero ( $s = 0$ ) implying no treatment ( $T_i = 0$ ). This implies that this cell is located outside the protected areas defined by CFP.

To estimate the local average treatment effects (LATE)  $\tau_h$  of the REDD+ PAs on cell<sub>i</sub> deforestation rate conditional on bandwidth choice  $h$ , I will follow Cattaneo, Idrobo, and Titiunik

(2019) which proposes a non-parametric method to identify the LATE parameter. I will add covariates which should not change the LATE magnitude but add precision to the estimator, the errors are clustered at X by X km grid groups. The reduced form estimation is the following:

$$y_i(h) = \alpha + \tau_h T_i + \beta_{1,h} f(X_i - c) + Z_i' \gamma + \epsilon_i \quad (B.3)$$

Where  $y_i$  corresponds to cell  $i$  deforestation,  $\tau_h$  is the average treatment effect of the CFP-protected areas,  $T_i$  is a dummy variable equal to 1 if the cell is within the borders of the PAs areas. The  $h$  parameter indicates that the estimation is performed conditional on cells being located within the optimal bandwidth  $h$ . In conclusion,  $f(X_i - c)$  is a functional form used to fit the data variation, and  $Z_i$  is a vector of cell characteristics as terrain, institutional, and infrastructure information.

The effects of interest ( $\tau$ ) is identified by the following:

$$\tau = E[Y(1) - Y(0)|X = c] = \lim_{x \downarrow c} E[Y|X = x] - \lim_{x \uparrow c} E[Y|X = x] \quad (B.4)$$

This indicates that the local average treatment effect of CFP ( $\tau$ ) can be identified by the difference between deforestation rates of treated cells (protected areas) and control cells (unprotected areas) around the cutoff  $c$ . The limit indicates that this parameter is the vertical difference between observations at the cutoff. This relies on a potential outcomes framework that, under the RDD assumptions, implies that  $Y(0)$  are proper counterfactual for  $Y(1)$  outcomes without the establishment of the new protected areas.

Furthermore, I verify heterogeneous effects estimated by cell subgroups as suggested by Cattaneo, Idrobo, and Titiunik (2019). This consists of estimating different local treatment effects ( $\tau_g$ ) for cells conditional on different subgroups ( $g$ ) defined by cell characteristics in the baseline year 2015. Exploring the USAID surveys, I will test heterogeneous effects for cell proximity to treated villages, and villages/chiefdom characteristics related to forest dependence and social norms. Using supplementary data I will check for effects conditional on road and infrastructure proximity to account for market access and different costs of deforestation. Using remote data on land characteristics such as slope, soil quality, and agriculture feasibility, I test how these effects differ conditional on terrain characteristics.

To test if the RDD identification assumptions hold, I perform a series of validation and

falsification tests proposed by (Cattaneo, Idrobo, and Titiunik 2019). I verify the covariate's continuous assumption around the cutoff and some placebo outcome tests. This aims to verify if the discontinuity observed around the cutoff only applies to deforestation rates. If there are substantial discontinuities on covariates, this indicates that there are other aspects that can impact the different levels of deforestation observed between areas. For the placebo outcomes test, if there are discrete jumps on outcomes not related to the objectives of the program (for example, soil agriculture feasibility) this would indicate that other aspects are influencing the context during the program period. I also test results sensibility to cutoff and bandwidth choices, and frequency of observations around the optimal cutoff.

**Village level outcomes** To estimate the program effect on village outcomes, I will use a Difference-in-Differences (DiD) approach. The exogeneity assumption is that the deforestation rates would keep the same trend for treatment and control in the absence of the program. The geographic unit of analysis is the surrounding of the villages surveyed by USAID. I choosed a 5 km buffer due the report of the majority of household on forest access. In the household survey, 90 % of the surveyed hhs report less than 5 km from the forest used to collect or produce goods. Related to agriculture fields, y % report that these fields are h km from them. The same happens in the village headperson survey, where they report the distance to forests used by the community. This suggests that choosing a 5 km buffer around these villages is a reasonable assumption to capture effects due village behavior. However, I used different buffer size to verify if my results are sensitive to its extension. Another concerning about the buffer size is the possibility of having overlapping areas. To deal with this possibility, I assigned weights to cells that are around more than 1 village buffer. The weight is simple the inverse of the number of villages sharing a particular cell, i.e.  $1/\#ofvillages$ . I show that my results are not sensitive to using weights to measure deforestation rates.

I will leverage the proximity to the protected areas as an intensity of treatment, as the program may. The reduced form is estimated as follows:

$$y_{vy} = \beta_0 + \beta_1 CFP_{vy} + \alpha_y + \delta_v + \epsilon_{vt}, \quad (B.5)$$

where  $y$  corresponds to the environmental outcomes around village  $v$  in year  $y$ ,  $CFP_{vy}$  is dummy variable equal to 1 if the village is included in one of the treated chiefdom and is located within  $x$  km from the protected areas.  $\alpha_y$  and  $\delta_v$  are year and village fixed effects

included to control for time-invariant village and year characteristics that can impact environmental outcomes.  $\beta_1$  informs the impact of offering the CFP program to villages closer to the protected areas on environmental outcomes.

I also run an event study for the village level computing yearly coefficients for 5km buffers around treated villages. I estimate the following:

$$y_{ivct} = \alpha + \sum_k \beta_k \mathbb{I}(t = k) CFP_{vc} + \delta_t + \gamma_c + \epsilon_{ict}, \quad (B.6)$$

In this equation  $y_{ict}$  corresponds to inverse hyperbolic sine of tree cover loss within village  $i$  5km buffer in chiefdom  $c$  at year  $t$ . I regress this on yearly coefficients ( $\beta_k$ ) before and after the program implementation. The coefficients will give me the yearly cumulative effect of the program on deforestation outcomes. I use time ( $\delta_t$ ) and chiefdom ( $\gamma_c$ ) fixed effects to control for time-invariant unobservable characteristics that may impact tree cover loss.  $\epsilon_{ict}$  is a idiosyncratic error term, and I clustered errors at the chiefdom level to account for serial correlation between cells.

To test for heterogeneous effects, I will interact the CFP dummy with social norms and forest dependence variables. For social norms, I will estimate the following:

$$y_{vy} = \beta_0 + \beta_1 CFP_{vy} + \beta_2 Social\_Norms + \beta_3 CFP_{vy} \times Social\_Norms + \alpha_y + \epsilon_{vt} \quad (B.7)$$

For forest dependence, I will estimate the following:

$$\begin{aligned} y_{vy} = & \beta_0 + \beta_1 CFP_{vy} + \beta_2 Forest\_Dependence + \\ & \beta_3 CFP_{vy} \times Forest\_Dependence + \alpha_y + \epsilon_{vt} \end{aligned} \quad (B.8)$$

The standard errors are clustered at the village level to take into account serial correlation between.

## C Additional Results (Online)

In this section I will present more results

### C.1 Distributional analysis

In this section, I will discuss some descriptive facts about the environmental outcomes in Eastern Zambia. Specifically, I discuss deforestation rates and tree cover before the program implementation. I will proceed with the description using different types of geographical units, such as chiefdoms, villages, and REDD+ protected areas.

**Deforestation rates in Zambia** Figure 4 shows the distribution of 0.1 degree cell share of forest canopy, by chiefdom. On the x-axis, we have the share of forest canopy for 0.1-degree cells, on the y-axis I plot the proportion of cells for each share of forest bin. I also plot the mean share of forest canopy for each location.

These figures clarify how the classification of cells as forested depends on the minimum threshold of forest canopy for considering a cell as forested. The mean share of the canopy of these cells is between 18% and 28 %, with the distributions concentrated between 5% and 50%. This suggests that the vegetation in Eastern Zambia is mainly sparse forest.

Contributing to what was discussed before, figure ?? shows the distribution of cell proportion forested conditional on different minimum thresholds of tree canopy for forest categorization, by chiefdom. Focusing on the blue distributions, the minimum threshold is 10% of the forest canopy, a big proportion of the cell has more than half of the cell is considered as a forest. However, increasing the threshold shifts the distribution to the left, indicating that the proportion of cells with considerable forested shares almost disappears.

I also plotted the tree cover in 2000 around villages included in the USAID survey. Figure ?? shows the tree cover distribution around 5km buffers from villages, by distance from the protected areas. The figure suggests that villages 5-10 km from the borders of the protected areas has an slightly different distribution. This villages have more cell with higher shares of canopy.

An important measure related to deforestation is the number of fires alerts captured by satellites. Using the FIRMS NASA dataset I plot the distribution of the fires alerts by chiefdom in figure ???. The distributions show a seasonal trend concentrating fires alerts between June and November in all the chiefdoms. The same can be seen when plotting a distribution for all

the chiefdoms in figure ??.

## D Appendix Figures and Table (Online)

Table D.1: Impact of CFP on tree cover loss area in multiple measures : Contracted Chiefdoms

	ihs in m2	ihs in ha	$D_{it}^{2000}$	$D_{it}^{t-1}$	std	ihs in m2	ihs in ha	$D_{it}^{2000},$	$D_{it}^{t-1}$	std
Contracted Chiefdom	-0.005 (0.250)	-0.019 (0.018)	-0.050 (0.062)	-0.071 (0.071)	-0.107 (0.069)					
Contracted - Protected						-0.413** (0.187)	-0.039** (0.016)	-0.119** (0.056)	-0.146** (0.064)	-0.165** (0.065)
Contracted - Not Protected						0.479* (0.281)	0.004 (0.019)	0.032 (0.065)	0.019 (0.074)	-0.038 (0.072)
R <sup>2</sup>	0.08	0.06	0.04	0.04	0.04	0.09	0.06	0.04	0.04	0.04
Observations	2,596,332	2,596,332	2,596,332	2,596,306	2,596,332	2,596,332	2,596,332	2,596,332	2,596,306	2,596,332
Chiefdom FE	Yes	Yes	Yes	Yes	Yes	Yes	Yes	Yes	Yes	Yes
Year FE	Yes	Yes	Yes	Yes	Yes	Yes	Yes	Yes	Yes	Yes

Note: This table presents estimates of the impact of Community Forest Partnerships (CFP) on tree cover loss area, measured using different approaches. The inverse hyperbolic sine measures in meters and hectares are obtained by applying the function to the newly deforested area within  $0.01 \times 0.01$  grids each year. Annual deforestation rate is calculated relative to the forest stock in 2000 ( $D_{it}^{2000}$ ) and the previous year ( $D_{it}^{t-1}$ ). The standard deviation of the newly deforested area is the outcome for the columns std. Columns 1 to 5 show the regression results for Contracted Chiefdom Grids, not distinguished by protection status. Columns 6 to 10 show the coefficients for protected and non-protected areas obtained in a regression that separates chiefdom cells into these categories. The control Grids include all areas outside the corridor indicated by the green group in Figure 5. Standard deviations are reported in parentheses, and errors are clustered at the chiefdom level. \*, \*\*, \*\*\* denote statistical significance at the 10%, 5%, and 1% level, respectively.

Table D.2: Impact of CFP on tree cover loss area in multiple measures: Protected and Non-Protected Matched samples

	ihs in m2	ihs in ha	$D_{it}^{2000}$	$D_{it}^{t-1}$	std	ihs in m2	ihs in ha	$D_{it}^{2000}$	$D_{it}^{t-1}$	std
Contracted - Protected	-0.360** (0.179)	-0.046*** (0.017)	-0.164*** (0.060)	-0.187*** (0.068)	-0.227*** (0.078)					
Contracted - Not Protected						0.271 (0.346)	-0.014 (0.027)	-0.057 (0.105)	-0.035 (0.092)	-0.112 (0.106)
R <sup>2</sup>	0.06	0.06	0.04	0.04	0.04	0.08	0.07	0.04	0.04	0.04
Observations	367,287	367,287	367,287	367,287	367,287	333,546	333,546	333,546	333,546	333,546
Chiefdom FE	Yes	Yes	Yes	Yes	Yes	Yes	Yes	Yes	Yes	Yes
Year FE	Yes	Yes	Yes	Yes	Yes	Yes	Yes	Yes	Yes	Yes

Note: This table presents estimates of the impact of Community Forest Partnerships (CFP) on tree cover loss area, measured using different approaches. The inverse hyperbolic sine measures in meters and hectares, are obtained by applying the function to the newly deforested area within  $0.01 \times 0.01$  grids each year. Annual deforestation rate is calculated relative to the forest stock in 2000 ( $D_{it}^{2000}$ ) and the previous year ( $D_{it}^{t-1}$ ). The standard deviation of the newly deforested area is the outcome for the columns std. Columns 1 to 5 show the regression results for Protected Grids, and columns 6 to 10 show the coefficients for Non-Protected Grids. The control Grids include all matched Grids outside the corridor indicated by the green group in Figure 6. Standard deviations are reported in parentheses, and errors are clustered at the chiefdom level. \*, \*\*, \*\*\* denote statistical significance at the 10%, 5%, and 1% level, respectively.

Table D.3: Impact of CFP on tree cover loss area in multiple measures: Non-Contracted Chiefdoms

	IHS in m2	IHS in ha	$D_{it}^{2000}$	$D_{it}^{t-1}$	std	IHS in m2	IHS in ha	$D_{it}^{2000}$	$D_{it}^{t-1}$	std
Non-Contracted Chiefdom	-0.189 (0.249)	-0.017 (0.022)	-0.043 (0.076)	-0.058 (0.087)	-0.098 (0.080)					
Non Contracted - Close						-0.260 (0.236)	-0.032* (0.018)	-0.102* (0.060)	-0.128* (0.069)	-0.154** (0.069)
Non Contracted - Far						-0.122 (0.357)	-0.003 (0.032)	0.012 (0.110)	0.006 (0.126)	-0.046 (0.109)
R <sup>2</sup>	0.09	0.07	0.04	0.04	0.04	0.09	0.07	0.04	0.04	0.04
Observations	2,868,238	2,868,238	2,868,238	2,868,212	2,868,238	2,868,238	2,868,238	2,868,238	2,868,212	2,868,238
Chiefdom FE	Yes	Yes	Yes	Yes						
Year FE	Yes	Yes	Yes	Yes						

Note: This table presents estimates of the impact of Community Forest Partnerships (CFP) on tree cover loss area, measured using different approaches. The inverse hyperbolic sine measures in meters and hectares are obtained by applying the function to the newly deforested area within  $0.01 \times 0.01$  grids each year. Annual deforestation rate is calculated relative to the forest stock in 2000 ( $D_{it}^{2000}$ ) and the previous year ( $D_{it}^{t-1}$ ). The standard deviation of the newly deforested area is the outcome for the columns std. Columns 1 to 5 show the regression results for Non-Contracted Chiefdom Grids, not distinguished by distance. Columns 6 to 10 show the coefficients for Grids less than 60 km and at least 60 km further from Protected Areas. The control Grids include all areas outside the corridor indicated by the green group in Figure 5. Standard deviations are reported in parentheses, and errors are clustered at the chiefdom level. \*, \*\*, \*\*\* denote statistical significance at the 10%, 5%, and 1% level, respectively.

Table D.4: Impact of CFP on tree cover loss area in multiple measures: Close and Far Matched samples

	IHS in m2	IHS in ha	$D_{it}^{2000}$	$D_{it}^{t-1}$	std	IHS in m2	IHS in ha	$D_{it}^{2000}$	$D_{it}^{t-1}$	std
Non Contracted - Close	-0.369 (0.262)	-0.046** (0.021)	-0.157** (0.072)	-0.186** (0.081)	-0.218** (0.086)					
Non Contracted - Far						-0.225 (0.376)	-0.014 (0.033)	-0.029 (0.117)	-0.040 (0.134)	-0.096 (0.119)
R <sup>2</sup>	0.09	0.06	0.04	0.04	0.03	0.10	0.08	0.05	0.05	0.05
Observations	611,662	611,662	611,662	611,662	611,662	656,696	656,696	656,696	656,696	656,696
Chiefdom FE	Yes	Yes	Yes	Yes	Yes	Yes	Yes	Yes	Yes	Yes
Year FE	Yes	Yes	Yes	Yes	Yes	Yes	Yes	Yes	Yes	Yes

Note: This table presents estimates of the impact of Community Forest Partnerships (CFP) on tree cover loss area, measured using different approaches. The inverse hyperbolic sine measures in meters and hectares are obtained by applying the function to the newly deforested area within  $0.01 \times 0.01$  grids each year. Annual deforestation rate is calculated relative to the forest stock in 2000 ( $D_{it}^{2000}$ ) and the previous year ( $D_{it}^{t-1}$ ). The standard deviation of the newly deforested area is the outcome for the columns std. Columns 1 to 5 show the regression results for Grids less than 60 km from Protected Areas. Columns 6 to 10 show the coefficients for Grids at least 60 km further from Protected Areas. The control Grids include all matched Grids outside the corridor indicated by the green group in Figure 6. Standard deviations are reported in parentheses, and errors are clustered at the chiefdom level. \*, \*\*, \*\*\* denote statistical significance at the 10%, 5%, and 1% level, respectively.

Table D.5: Summary statistics by Province

	Central	Copperbelt	Eastern	Luapula	Lusaka	Muchinga	North-Western	Northern	Southern	Western	Zambia
Cell canopy share in 2000 (%)	21.319 (9.80)	37.278 (13.15)	20.571 (8.75)	34.473 (24.70)	18.866 (7.83)	21.944 (12.36)	42.132 (14.88)	24.250 (16.32)	11.765 (5.96)	15.723 (11.19)	24.717 (16.49)
Tree cover in 2000 (ha)	30.198 (14.31)	52.572 (19.91)	29.094 (12.94)	48.634 (35.42)	26.584 (11.70)	31.317 (17.97)	59.973 (22.17)	34.523 (23.49)	16.733 (8.68)	22.393 (8.68)	35.101 (16.10)
Tree cover loss in ha (2001-2014)	1.085 (2.44)	4.641 (8.16)	0.940 (1.84)	2.529 (5.14)	0.514 (1.57)	0.611 (1.39)	1.684 (4.62)	1.064 (2.98)	0.377 (0.83)	0.742 (2.46)	1.219 (3.50)
Average rate of tree cover loss (2001-2014)	0.034 (0.06)	0.087 (0.13)	0.034 (0.06)	0.044 (0.07)	0.021 (0.05)	0.018 (0.04)	0.027 (0.07)	0.027 (0.05)	0.024 (0.05)	0.025 (0.06)	0.030 (0.07)
Altitude (m)	1129.938 (197.01)	1241.392 (57.15)	862.928 (206.49)	1177.494 (122.07)	856.272 (277.30)	1123.954 (303.27)	1223.777 (113.32)	1283.849 (193.85)	1018.425 (215.68)	1071.827 (60.67)	1120.530 (217.59)
Maize Potential Yield (kg/acre)	2942.332 (406.83)	3062.984 (82.12)	3109.202 (143.69)	2954.047 (132.21)	2993.621 (138.96)	2868.563 (357.14)	3060.152 (228.24)	2776.137 (410.42)	3045.641 (161.61)	3252.409 (181.82)	3017.646 (310.06)
Observations	92898	26441	43443	42142	22036	73077	105605	64802	57976	108277	636697

Note: This table present summary statistics for Provinces in Zambia. The table present the mean value for cells within GMAs and PAs, with exception of Tree cover loss in ha, which corresponds to the sum of tree cover loss in HA for a given  $0.01 \times 0.01$  cells. Standard errors are presented in parentheses.